

Increased Lipid Synthesis and Decreased β -Oxidation in the Liver of SHR/NDmcr-cp (*cp/cp*) Rats, an Animal Model of Metabolic Syndrome

Shizuyo Tanaka · Tohru Yamazaki · Satoshi Asano · Atsushi Mitsumoto · Daisuke Kobayashi · Naomi Kudo · Yoichi Kawashima

Received: 5 April 2013 / Accepted: 24 August 2013 / Published online: 18 September 2013
© AOCs 2013

Abstract SHR/NDmcr-cp (*cp/cp*) rats (SHR/NDcp) are an animal model of metabolic syndrome. A previous study of ours revealed drastic increases in the mass of palmitic (16:0), oleic (18:1n-9), palmitoleic (16:1n-7), *cis*-vaccenic (18:1n-7) and 5,8,11-eicosatrienoic acids in the liver of SHR/NDcp. However, detailed information on the class of lipid accumulated and the mechanism responsible for the overproduction of the accumulated lipid in the liver was not obtained. This study aimed to characterize the class of lipid accumulated and to explore the mechanism underlying the lipid accumulation in the liver of SHR/NDcp, in comparison with SHR/NDmcr-cp (+/+) (lean hypertensive littermates of SHR/NDcp) and Wistar Kyoto rats. In the liver of SHR/NDcp, *de novo* synthesis of fatty acids (16:0, 18:1n-9 and 16:1n-7) and triacylglycerol (TAG) synthesis were up-regulated and fatty acid β -oxidation was down-regulated. These perturbations of lipid metabolism caused fat accumulation in hepatocytes and accumulation of TAG, which were enriched with 16:0, 18:1n-9 and 16:1n-7, in the liver of SHR/NDcp. On the other hand, no changes were found in hepatic contents of diacylglycerol and unesterified fatty acid (FFA); among FFA, there were no differences in

the hepatic concentrations of unesterified 16:0 and stearic acid between SHR/NDcp and two other groups of rats. Moreover, little change was brought about in the expression of genes responsive to endoplasmic reticulum stress in the liver of SHR/NDcp. These results may reinforce the pathophysiological role of stearyl-CoA desaturase 1 and fatty acid elongase 6 in the liver of SHR/NDcp.

Keywords Hepatic TAG accumulation · MUFA · *De novo* lipogenesis · β -Oxidation · SHR/NDmcr-cp (*cp/cp*) rat

Abbreviations

ACC1	Acetyl-CoA carboxylase 1
ACLY	ATP-citrate lyase
ACSL	Long-chain acyl-CoA synthetase
ATGL	Adipose triglyceride lipase
BSA	Bovine serum albumin
CGI-58	Comparative gene identification-58
CHOP	CCAAT/enhancer binding protein homologous protein
ChREBP	Carbohydrate responsive element-binding protein
CPT1a	Carnitine palmitoyltransferase 1a
DGAT	Acyl-CoA:diacylglycerol acyltransferase
EDTA	Ethylenediaminetetraacetic acid
Elovl	Fatty acid elongase
ER	Endoplasmic reticulum
FABP1	Fatty acid binding protein 1
FABPpm	Plasma membrane-associated fatty acid binding protein
Fads	Fatty acid desaturase
FAS	Fatty acid synthase
FAT/CD36	Fatty acid translocase
FATP	Fatty acid transport protein

S. Tanaka · T. Yamazaki · D. Kobayashi · N. Kudo · Y. Kawashima (✉)

Faculty of Pharmaceutical Sciences, Josai University,
1-1 Keyakidai, Sakado, Saitama 350-0295, Japan
e-mail: ykawash@josai.ac.jp

S. Asano

Department of Pharmaceutical Sciences, International University
of Health and Welfare, 2600-1 Kitakanemaru, Ohtawara,
Tochigi 324-8501, Japan

A. Mitsumoto

Faculty of Pharmaceutical Sciences, Josai International
University, 1 Gumyo, Togane, Chiba 283-8555, Japan

GPAT	Glycerol-3-phosphate acyltransferase
GRP78	Glucose-regulated protein 78 kDa
H&E	Hematoxylin and eosin
HOMA-IR	Homeostatic model of insulin-resistance index
LPK	L-type pyruvate kinase
LCAD	Long-chain acyl-CoA dehydrogenase
LXR α	Liver X receptor α
MCAD	Medium-chain acyl-CoA dehydrogenase
ME1	Malic enzyme 1
MS	Metabolic syndrome
NAFLD	Nonalcoholic fatty liver disease
ORO	Oil Red O
PCE	Palmitoyl-CoA chain elongation
PCR	Polymerase chain reaction
PEPCK	Phosphoenolpyruvate carboxykinase
PPAR α	Peroxisome proliferator-activated receptor α
SCD	Stearoyl-CoA desaturase
SHR	Spontaneously hypertensive rats
SHR/ND+	SHR/NDmcr-cp (+/+) rats
SHR/NDcp	SHR/NDmcr-cp (<i>cp/cp</i>) rats
SHRSP	Stroke-prone spontaneously hypertensive rats
SREBP-1c	Sterol regulatory element binding protein-1c
s-XBP1	Spliced X-box binding protein 1
TLC	Thin-layer chromatography
VLCAD	Very long-chain acyl-CoA dehydrogenase
WKY	Wistar Kyoto rats

Introduction

Metabolic syndrome (MS) is a cluster of metabolic abnormalities, including visceral obesity, glucose intolerance, hypertension, and dyslipidemia with underlying insulin resistance. The coexistence of these disorders is considered to be increasingly linked to cardiovascular diseases. Several animal models of MS have been presented. One of these is SHR/NDmcr-cp (*cp/cp*) rats (SHR/NDcp). SHR/NDcp are an inbred subline of SHR/National Institute of Health (NIH)-corpulent rats [1]; namely, SHR/NIH-corpulent rats are bred by the Disease Model Cooperative Association (Dmcr), Japan, and the rats are named SHR/NDmcr-cp. Spontaneously hypertensive rats (SHR) were spontaneously developed as a colony from normotensive Wistar Kyoto rats (WKY) [2]. By crossing SHR with Sprague–Dawley rats, obese spontaneously hypertensive rats were obtained and named Koletsky rats, which were thought to be heterozygous for a recessive fatty (*fa*) gene [3]. The noncorpulent genes of this strain were eliminated by mating the rats with SHR, and the obtained rats were designated as SHR/NIH-corpulent rats [4]. SHR/

NIH-corpulent rats are a congenic rat strain that has the genetic background of SHR and inherits obese characteristics from Koletsky rats, which have been demonstrated to carry a nonsense mutation in the leptin receptor gene [5]. Thus, SHR/NDcp as well as SHR/NIH-corpulent rats have corpulent “*cp*” gene(s), display visceral obesity, dyslipidemia and glucose intolerance in addition to hypertension and, therefore, constitute an animal model of MS [6, 7]. The gene currently established as the corpulent “*cp*” gene is the leptin receptor gene; however, the implications of other genes reflecting obesity and other symptoms of MS in this rat remain to be resolved.

The liver is a major determinant of whole-body fatty acid and neutral lipid metabolism, and fatty liver is considered as the hepatic manifestation of MS [8]. Moreover, fatty acid species that exist in the liver are pathophysiologically critical [9–11]. Therefore, in a previous study, we compared the fatty acid profile of hepatic lipids among SHR/NDcp, WKY, SHR, stroke-prone spontaneously hypertensive rats (SHRSP) and SHR/NDmcr-cp (+/+) rats (SHR/ND+) (lean hypertensive littermates of SHR/NDcp), and demonstrated that SHR/NDcp and the other four strains and/or substrains of rats were clearly disparate in terms of fatty acid profile [12]. This disparity was due to drastic increases in the mass of palmitic (16:0), oleic (18:1n-9), palmitoleic (16:1n-7), *cis*-vaccenic (18:1n-7) and 5,8,11-eicosatrienoic (20:3n-6) acids in the liver of SHR/NDcp. These findings are strongly suggestive of excessive lipid accumulation in the liver of SHR/NDcp. However, detailed characterization of the class of lipid accumulated in the liver of SHR/NDcp has not been performed; moreover, the mechanism underlying the overproduction of hepatic steatosis-related lipids is still unclear. This information is required to establish SHR/NDcp as a useful model of MS. In this context, the aims of this study were (1) to characterize the class of lipid accumulated in the liver and (2) to explore the mechanism underlying the lipid accumulation in the liver of SHR/NDcp, in comparison with SHR/ND+ and WKY. The present study showed that *de novo* synthesis of fatty acids (16:0, 18:1n-9 and 16:1n-7) and triacylglycerol (TAG) synthesis were up-regulated and fatty acid β -oxidation was down-regulated in the liver of SHR/NDcp; these perturbations of lipid metabolism caused fat accumulation in hepatocytes and accumulation of TAG, which were enriched with 16:0, 18:1n-9 and 16:1n-7. On the other hand, no changes were found in the hepatic contents of diacylglycerol (DAG) and unesterified fatty acid (FFA). Among FFA, there were no differences in the hepatic concentrations of 16:0 and stearic acid (18:0) among SHR/NDcp, SHR/ND+ and WKY, and little change was brought about in expression of genes responsive to endoplasmic reticulum (ER) stress in the liver of SHR/NDcp. The pathophysiological significance of up-

regulation of stearoyl-CoA desaturase (SCD) 1 and fatty acid elongase (Elovl) 6 in the liver of SHR/NDcp is discussed.

Materials and Methods

Materials

The following materials were obtained from the indicated commercial sources: [$1\text{-}^{14}\text{C}$]16:0 (56.0 Ci/mol) and [$1\text{-}^{14}\text{C}$]18:1n-9 (55.0 Ci/mol) (American Radiolabeled Chemicals, Inc., St. Louis, MO, USA); L-[$U\text{-}^{14}\text{C}$]glycerol-3-phosphate (159 Ci/mol) and [$2\text{-}^{14}\text{C}$]malonyl-CoA (56.0 Ci/mol) (GE Healthcare, Little Chalfont, Buckinghamshire, UK); [$1\text{-}^{14}\text{C}$]palmitoyl-CoA (60.0 Ci/mol) (Moravék Biochemicals, Inc., Brea, CA, USA); acetyl-CoA, malonyl-CoA, palmitoyl-CoA, stearoyl-CoA, glycerol-3-phosphate and bovine serum albumin (BSA) (essentially fatty acid free for enzyme assays and fraction V for protein assay) (Sigma Aldrich Japan, Tokyo, Japan); 1,2-dioleoyl-*sn*-glycerol (Doosan Serdary Research Laboratories, Etobicoke, Ontario, Canada); rat insulin RIA kit (Millipore Corp., Billerica, MA, USA); sterol regulatory element binding protein-1c (SREBP-1c) antibody (2A4) (Santa Cruz Biotechnologies Inc., Santa Cruz, CA, USA); and anti-mouse IgG horseradish peroxidase-linked antibody (Cell Signaling, Danvers, MA, USA).

Animals

All animal procedures were approved by Josai University's Institutional Animal Care Committee in accordance with the Guidelines for Proper Conduct of Animal Experiments (Science Council of Japan). Fifteen-week-old male WKY, SHR/ND+ and SHR/NDcp were obtained from SLC (Hamamatsu, Japan). The animals were fed on a standard diet (CE-2; Clea Japan, Tokyo, Japan) *ad libitum* and allowed free access to water. The fatty acid composition (in mol%) of the standard diet was as follows: 16:0, 23.2 %; 16:1n-7, 2.0 %; 18:0, 2.4 %; 18:1n-9, 19.7 %; 18:1n-7, 2.2 %; linoleic acid (18:2n-6), 42.1 %; α -linolenic acid (18:3n-3), 3.6 %; arachidonic acid (20:4n-6), 0.2 %; 5,8,11,14,17-eicosapentaenoic acid (20:5n-3), 2.9 %; 7,10,13,16,19-docosapentaenoic acid (22:5n-3), 0.3 %; and 4,7,10,13,16,19-docosahexaenoic acid (22:6n-3), 1.3 %. After acclimatization, at the age of 22 weeks, rats were anesthetized with diethyl ether, and blood was withdrawn from the inferior vena cava. The liver was rapidly removed, washed with saline and weighed. Livers were used for histopathological analyses, analyses of lipids and glycogen, preparations of cytosol, microsomes and nuclear extracts, and preparation of liver slices. The portions of livers that

were used for preparing cytosol and microsomes were perfused with ice-cold saline. To estimate the homeostatic model of insulin-resistance index (HOMA-IR), some rats were starved for 12 h and plasma was prepared from blood.

Histopathological Analyses

Isolated livers were fixed in 10 % neutral-buffered formalin, embedded in paraffin wax, sectioned (3–4 μm thick) and stained with hematoxylin and eosin (H&E). To visualize fat deposition in the liver, frozen sections (10–12 μm thick) were cut in a cryostat and stained with Oil Red O (ORO) and with hematoxylin. The sections were evaluated by scanning the entire tissue specimen under low-power magnification (40 \times) and then confirmed under higher power magnification (100 \times , 200 \times and 400 \times). All histopathological scoring and evaluation was carried out by blind evaluation without knowledge of the treatment. Images were obtained under a light microscope (Olympus BX51; Olympus, Tokyo, Japan) equipped with a DP50 digital camera (Olympus).

Lipid Analyses

To determine the acyl composition of lipid classes, total lipid was extracted from portions of livers by the method of Bligh and Dyer [13], after the additions of known amounts of nonadecanoic acid, cholesteryl heptadecanoate and triheptadecanoin as internal standards. Cholesteryl ester (CE), TAG, FFA, DAG and phospholipid (PL) were separated by thin-layer chromatography (TLC) on silica gel G plates, which were developed with *n*-hexane/diethyl ether/acetic acid (80:30:1, by vol.). The separated lipids were extracted from silica gel as described previously [14]; DAG and PL were extracted from silica gel after the addition of known amounts of methyl heptadecanoate as internal standards. The acyl composition of these lipids was determined as the methyl esters of fatty acids by gas chromatography (Shimadzu GC-2014; Shimadzu, Kyoto, Japan) [15]. To determine the acyl composition of the subclass of microsomal PL, total lipid was extracted from microsome suspensions [13]. Phosphatidylcholine (PtdCho), phosphatidylethanolamine (PtdEtn) and other lipids were separated by TLC on silica gel G plates, which were developed with chloroform/methanol/acetic acid/water (100:75:7:4, by vol.). The acyl composition of these PL was determined as the methyl esters of fatty acids by gas chromatography.

Biochemical Parameters

Total lipid was extracted from portions of livers [13]. Cholesterol and lipid phosphorus was measured as reported previously [16, 17]. TAG, which was separated by TLC

and extracted from silica gel, was determined using Triglyceride E-Test Wako (Wako Pure Chemicals, Osaka, Japan) [18]. Glycogen contents in the livers were measured by the enzymatic method as described previously [19]. Concentrations of glucose and insulin in plasma from fasted rats were determined by Glucose CII-test Wako (Wako Pure Chemicals) and rat insulin RIA kit, respectively, and HOMA-IR was calculated.

mRNA Expression

mRNA expression was analyzed by real-time quantitative PCR as described previously [12].

The sequences of primers used in this study are listed in Table 1. X-box binding protein 1 (XBP1) mRNA splicing was analyzed as reported previously [20]; PCR products were separated by electrophoresis in 2.5 % agarose gels and visualized by ethidium bromide staining.

Enzyme Assays

One portion of the perfused livers was homogenized with 1.5 volumes of a phosphate–bicarbonate buffer (70 mM KHCO_3 /85 mM K_2HPO_4 /9 mM KH_2PO_4 /1 mM dithiothreitol) (pH 8.0) in a Potter glass-Teflon homogenizer. The homogenates were centrifuged at $20,000\times g$ for 10 min, and the supernatant was then centrifuged at $105,000\times g$ for 60 min. The resulting supernatant was used as cytosol. The other portion of the perfused livers was used for preparing microsomes as described previously [14]. All operations were carried out at 0–4 °C. Protein concentrations in the preparations were determined by the method of Lowry et al. [21] using BSA as a standard. The activity of fatty acid synthase (FAS) in cytosol was determined as the rate of NADPH oxidation [22]. The activities of SCD in microsomes were determined as described previously [14] and the activity is presented as the rate constant (k^+) for stearoyl-CoA-stimulated re-oxidation of NADH-reduced cytochrome b_5 . Palmitoyl-CoA chain elongation (PCE) in microsomes was assayed using palmitoyl-CoA and [2- ^{14}C]malonyl-CoA, as described previously [23]. The activity of long-chain acyl-CoA synthetase (ACSL) in microsomes was assayed using [^{14}C]16:0 [24]. Glycerol-3-phosphate acyltransferase (GPAT) activity in microsomes was determined using palmitoyl-CoA and [^{14}C]glycerol-3-phosphate [25]. Acyl-CoA:diacylglycerol acyltransferase (DGAT) in microsomes was assayed using [1- ^{14}C]palmitoyl-CoA and dioleoylglycerol [26].

Nuclear Extracts and Western Blot Analyses

Nuclear extracts of livers were prepared according to Sheng et al. [27]. Briefly, portions of the livers were

homogenized in 10 volumes of buffer A (10 mM Hepes (pH 7.6) containing 25 mM KCl, 1 mM EDTA, 2 M sucrose, 10 % (v/v) glycerol, 0.15 mM spermine and 2 mM spermidine) supplemented with protease inhibitors (*N*-acetyl-leucylleucylnorleucinal at 50 $\mu\text{g}/\text{mL}$, 0.1 mM Pefabloc, pepstatin A at 5 $\mu\text{g}/\text{mL}$, leupeptin at 10 $\mu\text{g}/\text{mL}$ and aprotinin at 2 $\mu\text{g}/\text{mL}$) using a Potter glass-Teflon homogenizer. The homogenate (10 mL) was layered over 10 mL of buffer A in a RPS-27 rotor (Hitachi Koki, Tokyo, Japan) and centrifuged at $77,000\times g$ for 60 min at 4 °C. The resulting nuclear pellet was resuspended in 0.4 mL of 10 mM Hepes buffer (pH 7.6) containing 100 mM KCl, 2 mM MgCl_2 , 1 mM EDTA, 1 mM dithiothreitol and 10 % (v/v) glycerol supplemented with proteinase inhibitors, after which 0.04 mL of 4 M ammonium sulfate (pH 7.9) was added. Each mixture was centrifuged at $266,000\times g$ in a S120AT2 rotor (Hitachi Koki) for 45 min at 4 °C. The supernatant was used as nuclear extract. Protein concentrations in the nuclear extracts were measured by dye protein assay (BioRad, Hercules, CA, USA).

Samples containing 7.5–30 μg of protein were boiled in 0.063 M Tris–HCl (pH 6.8) containing 5 % (v/v) 2-mercaptoethanol, 2 % sodium dodecyl sulfate, 6 % (v/v) glycerol and 0.002 % bromophenacylblue. The denatured samples were separated by sodium dodecyl sulfate/polyacrylamide gel electrophoresis on a 10 % gel and then transferred to a polyvinylidene difluoride membrane (BioRad) using a Trans-Blot Semi-Dry Electrophoretic Transfer Cell (BioRad). The membrane was blocked in Tris-buffered saline (pH 7.6) containing 0.1 % Tween-20, 5 % skim milk and 1 % BSA, and then incubated with mouse anti-SREBP-1c monoclonal antibody (1:500) overnight. The membrane was washed in Tris-buffered saline (pH 7.6) containing 0.1 % Tween-20, incubated with anti-mouse IgG horseradish peroxidase-linked antibody (1:2,000) for 4 h, and washed three times in Tris-buffered saline (pH 7.6) containing 0.1 % Tween-20. Proteins were visualized using the ECLplus kit (GE Healthcare) and detected in a LAS-1000 (GE Healthcare).

Ex Vivo Fatty Acid Esterification and Oxidation in Liver Slices

The rats were killed and their livers were quickly removed. The left lobe was separated, and precision-cut liver slices (200 μm thick; 75–85 mg) were prepared with a Krumdieck tissue slicer (Alabama Research Development, Munford, AL, USA) as described previously [28].

The rate of 18:1n-9 incorporation into lipids was determined essentially according to Iritani et al. [29] with some modifications. Liver slices were incubated in glass vials that contained 2 mL of Krebs–Henseleit buffer (pH 7.4), containing 5 mM glucose, 0.25 mM [1- ^{14}C]18:1n-9

Table 1 Sequences of primers used for real-time PCR

	Primer (5'–3')	Accession no.
Fatty acid synthase (FAS)	F: CGCCGACCAGTATAAAACCCA R: GTTGAATCGGCACCCAAGTC	M76767
Acetyl-CoA carboxylase 1 (ACC1)	F: AACGCCTTCACACCACCTTG R: AGTCGCAGAAGCAGCCCAT	J03808
ATP-citrate lyase (ACLY)	F: AAACGTATCGCCCAGGCAGT R: GTAACGCAGCACGTGATCCAT	J05210
Malic enzyme 1 (ME1)	F: ACAATACAGTTTGGCATTCCG R: AGGATTCGCTCTCCATCAGTCA	NM_012600
Stearoyl-CoA desaturase 1 (SCD1)	F: TCACCTTGAGAGAAGAATTAGCA R: TTCCCATTCCTTCACTCTGA	J02585
Fatty acid elongase 6 (Elov16)	F: AGAACACGTAGCGACTCCGAA R: CAAACGCGTAAGCCCAGAAT	AB071986
Acyl-CoA:diacylglycerol acyltransferase 1 (DGAT1)	F: CCGTGGTATCCTGAATTGGT R: GGCGCTTCTCAATCTGAAAT	NM_053437
Acyl-CoA:diacylglycerol acyltransferase 2 (DGAT2)	F: ATCTTCTCTGTCACCTGGCT R: ACCTTTCTTGGGCGTGTCC	NM_001012345
Glycerol-3-phosphate acyltransferase 1 (GPAT1)	F: AGACACAGGCAGGGAATCCAC R: AATTCCTGGAGAAGCCAG	AF021348
Glycerol-3-phosphate acyltransferase 4 (GPAT4)	F: TTGGAGTCTGGAATTTGCTGA R: GGCTAATCCCTGTGAATGCCA	NM_001047849
Fatty acid desaturase 1 (Fads1)	F: TACAGGCAACCTGCAACGTTT R: GGTGCCACCTTGTGGTAGTTGT	NM_053445
Fatty acid desaturase 2 (Fads2)	F: GCCACTTAAAGGGTGCCTCC R: TGCAGGCTCTTTATGTCGGG	BC081776
Fatty acid elongase 5 (Elov15)	F: ACCACCATGCCACTATGCTCA R: GGACGTGGATGAAGCTGTTG	AB071985
Fatty acid translocase (FAT/CD36)	F: CGAAGGCTTGAATCCTACCG R: TGTTGACCTGCAGTCGTTT	NM_031561
Fatty acid transport protein 2 (FATP2)	F: TTCAACAGTGGCGATCTCCTG R: ACCGGAAGGTGTCTCCAAT	NM_031736
Fatty acid transport protein 4 (FATP4)	F: CCTGGTGTACTATGGATTCCGC R: GCTGAAAACCTTCTCCGGATCA	NM_001100706
Fatty acid transport protein 5 (FATP5)	F: TTGCGAACGTACGGCAAGTAG R: AAGGCGGTCTCGGAAGTAGAAG	NM_024143
Plasma membrane-associated fatty acid binding protein (FABPpm)	F: TCTGCCAATCCTATGCCAA R: CACCCTTTTGGCTTCTTC	NM_013177
Fatty acid binding protein 1 (FABP1)	F: CGGCAAGTACCAAGTGCAGAG R: CTGACACCCCCTTGATGTCCT	BC086947
Long-chain acyl-CoA synthetase 1 (ACSL1)	F: TCAGAGCAGTTTCATCGGCATC R: GTCGGTTCCAAGCGTGCATA	NM_012820
Long-chain acyl-CoA synthetase 3 (ACSL3)	F: GGTGGCCAAAATGTGACAATG R: AAACCTCTCCAATATCGCCAGT	NM_057107
Long-chain acyl-CoA synthetase 5 (ACSL5)	F: CAAACATGGCTGCTTTCCTCA R: ACCCTGGACAAGCCTCTCAAA	NM_053607
Carnitine palmitoyltransferase 1a (CPT1a)	F: AAGGCAGCGTTCTTCGTGA R: GTCAAAAGCATCTTCCATGC	NM_031559
Medium-chain acyl-CoA dehydrogenase (MCAD)	F: CTTTGCCTCTATTGCGAAGGC R: TCCGAAAATCTGCACAGCATC	J02791

Table 1 continued

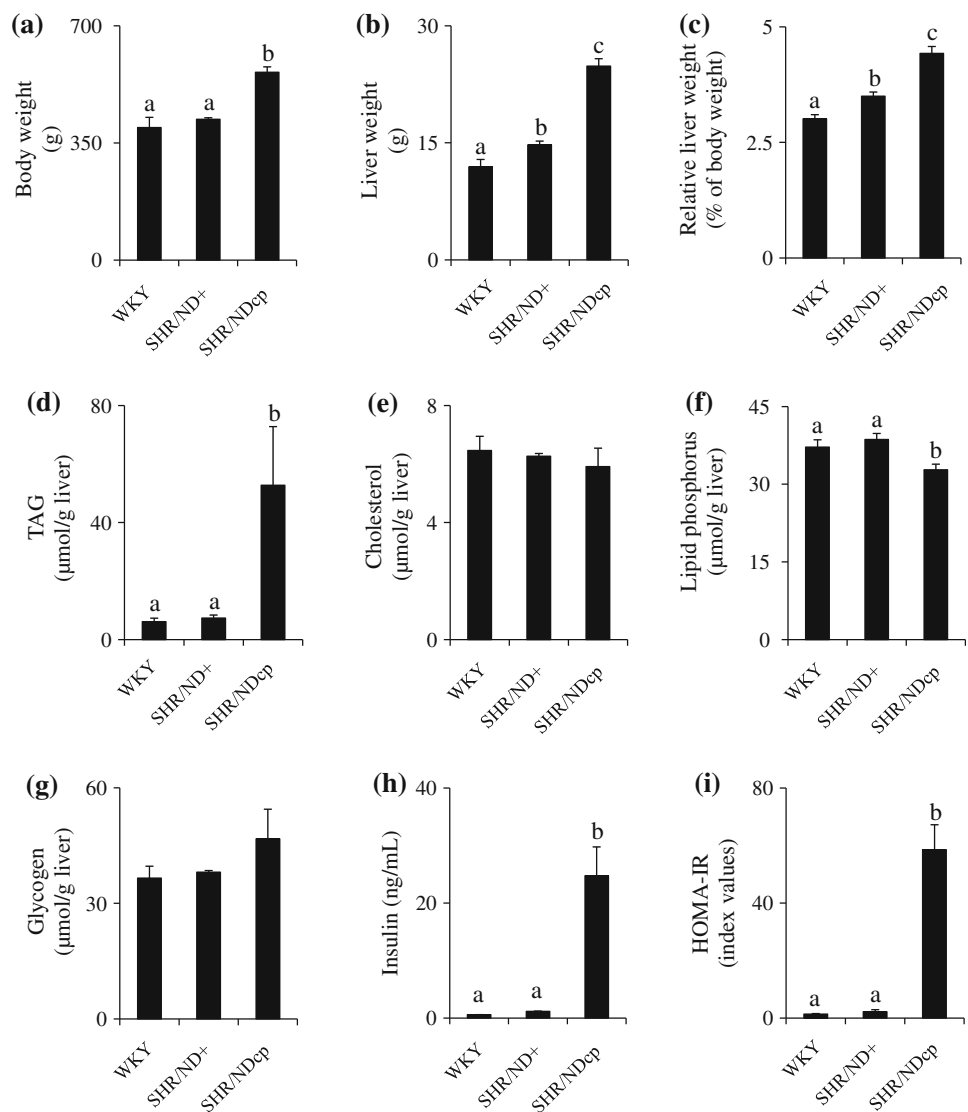
	Primer (5′–3′)	Accession no.
Long-chain acyl-CoA dehydrogenase (LCAD)	F: TGTATTGGTGCCATAGCCATGA R: CCCAGACCTTTTGGCATTGT	L11276
Very long-chain acyl-CoA dehydrogenase (VLCAD)	F: ACAGCTTTCGTAGTGAACGGA R: CTGGCACCTTGACTCCATCAA	D30647
Adipose triglyceride lipase (ATGL)	F: TCACCAACACCAGCATCCAA R: TCCATCTCGGTAGCCCTGTTT	NM_001108509
Comparative gene identification-58 (CGI-58)	F: TGCATAGATGGCAACTCTGGC R: ATACACATAATGCCCTGCCCC	NM_212524
L-Type pyruvate kinase (LPK)	F: TGTGTACCACCGCCAGTTGTT R: AGCACTGAAGGAAGCCTCCA	M17685
Phosphoenolpyruvate carboxykinase (PEPCK)	F: TGCCTGGATGAAGTTTGATG R: GCCCGGAGCAACTCCAAAAA	NM_198780
Sterol regulatory element binding protein-1c (SREBP-1c)	F: GGAGCCATGGATTGCACATT R: AGGAAGGCTTCCAGAGAGGA	AF286469
Carbohydrate responsive element-binding protein (ChREBP)	F: AATAGAGGAGCTCAATGCT R: CCCAGAACTTCCAGTTGTGC	AB074517
Peroxisome proliferator-activated receptor α (PPAR α)	F: AATGCCCTCGAACTGGATGAC R: CACAATCCCCTCCTGCAACTT	NM_013196
Liver X receptor α (LXR α)	F: CCACAGCTCAGCCCAGAA R: GCGGTGACTCGAAGTCGGT	NM_031627
Glucose-regulated protein 78 kDa (GRP78)	F: CCACCAGGATGCAGACATTG R: AGGGCCTCCACTTCCATAGAG	NM_013083
CCAAT/enhancer binding protein homologous protein (CHOP)	F: CTCTGCCTTTCGCCTTTGAG R: ATAGGTGCCCCCAATTTTCATC	U36994
X-box binding protein 1 (XBP1)	F: ACACGCTTGGGGATGAATG R: CCATGGGAAGATGTTCTGGG	NM_001004210
β -Actin	F: TGCAGAAGGAGATTACTGCC R: CGCAGCTCAGTAACAGTCC	V01217

(0.3 μ Ci) and 0.6 % BSA (essentially fatty acid-free) for 10 min at 37 °C under an O₂–CO₂ atmosphere (95:5, by vol.) with shaking (60 oscillations/min). At the end of the incubation, the liver slice was at once transferred to a new vial that contained 2 mL of the above-mentioned incubation medium (except for [¹⁴C]18:1n-9), which was chilled at 0 °C. Then, immediately, the liver slice was transferred to a glass vial containing chloroform/methanol/water (1:2:0.8, by vol.), and lipids were extracted with Polytron (PT10-35) (Kinematica AG, Luzern, Switzerland) according to Bligh and Dyer [13]. CE, TAG, FFA, DAG and PL were separated by TLC. The separated lipids were extracted from silica gel as described above. The extract was mixed with scintillation fluid, and the radioactivity was then measured using a liquid scintillation counter (Aloka LSC 6100; Hitachi-Aloka, Tokyo, Japan).

The rate of 16:0 oxidation was determined as described previously [30]. Liver slices were incubated in glass vials that contained 2 mL of Krebs–Henseleit buffer (pH 7.4) containing 5 mM glucose, 0.25 mM [1-¹⁴C]16:0 (0.3 μ Ci)

and 0.6 % BSA (essentially fatty acid-free) for 30 min at 37 °C under an O₂–CO₂ atmosphere (95:5, by vol.) with shaking (90 oscillations/min). The vials were capped with rubber stoppers from which were suspended plastic center-wells. The incubation was terminated by the injection of 1 mL of 0.6 M HClO₄ into the vial, and 0.2 mL of 1 M benzethonium hydroxide in methanol was injected into the center well. The vials were shaken (60 oscillation/min) for 45 min at room temperature to trap radio-labeled CO₂ into benzethonium hydroxide. Then, the content of the center well was transferred to a counting vial and mixed with scintillation fluid, and the radioactivity was measured using a liquid scintillation counter. The liver slice was homogenized with the incubation mixture that was acidified with HClO₄. After centrifugation at 1,500 \times g for 10 min, the resulting supernatant was neutralized with 5 M KOH, and then its pH was adjusted to 4 using 3 M acetate buffer (pH 4.0); the obtained aqueous phase was extracted five times with 5 mL of petroleum ether to remove traces of the [¹⁴C]16:0. An aliquot of the aqueous phase was mixed with

Fig. 1 Characteristics of SHR/NDcp. **a** Body weight, **b**, liver weight, **c** relative liver weight, **d** TAG in the liver, **e** cholesterol in the liver, **f** lipid phosphorus in the liver, **g** glycogen in the liver, **h** insulin in plasma, **i** HOMA-IR. Values represent mean \pm SD ($n = 4-8$). a, b, c Differences without a common superscript are statistically significant ($p < 0.05$). In the absence of a superscript, the differences in the means are not significant ($p > 0.05$)



scintillation fluid, and the radioactivity was determined as acid soluble oxidation products.

Statistical Analyses

Homogeneity of variance was established using one-way analysis of variance. When a difference was significant ($p < 0.05$), Scheffé's multiple range test was used as a post hoc test. The results were considered to be significant if the value of p was < 0.05 .

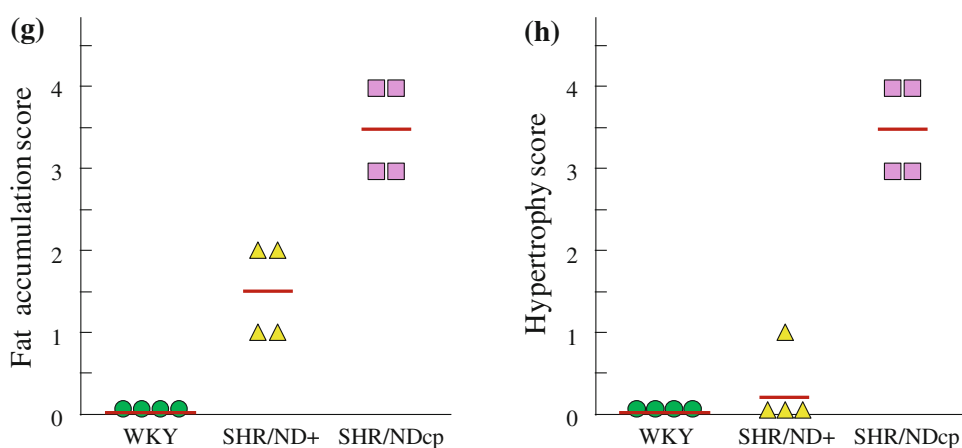
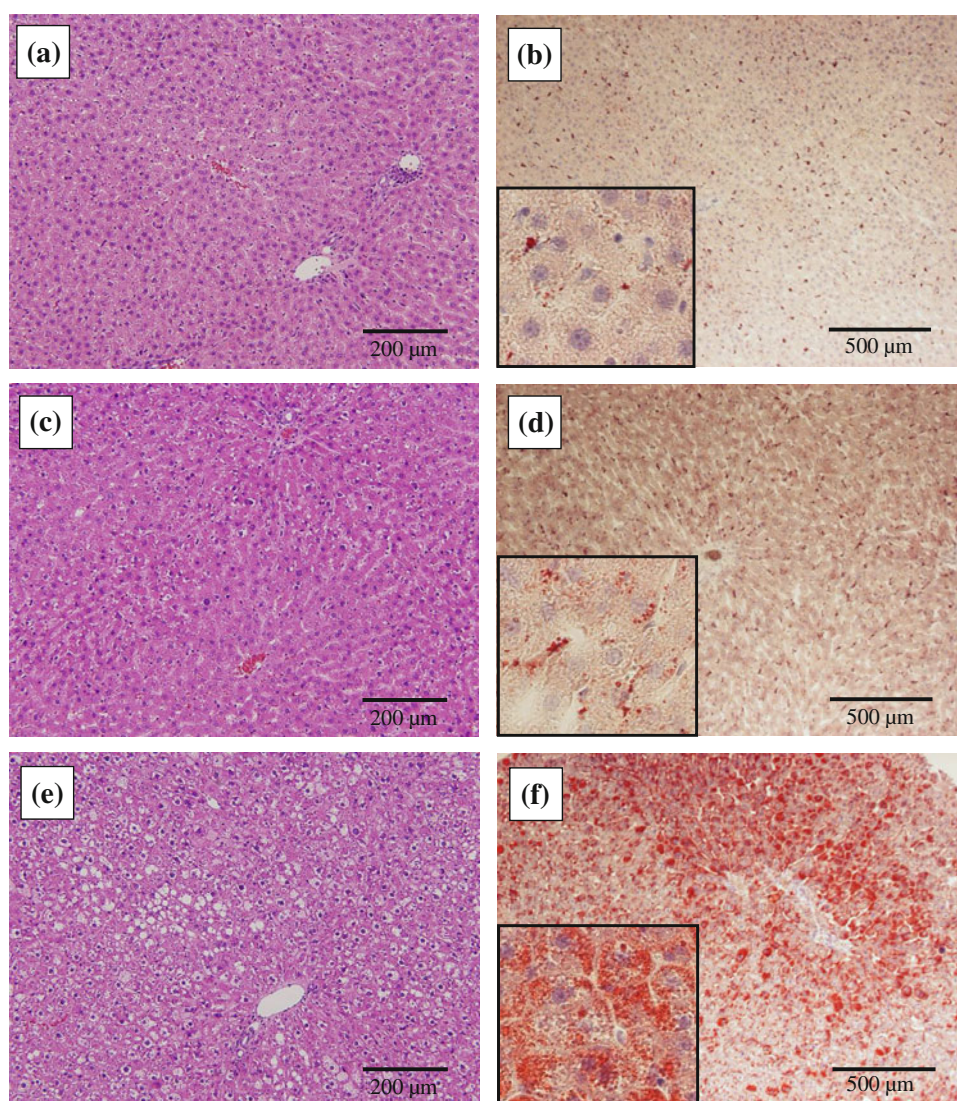
Results

Characteristics of SHR/NDcp

Body weights of SHR/NDcp were 142 % of those of WKY (Fig. 1a). Liver weights of SHR/NDcp were 2.1-fold of

those of WKY and relative liver weights of SHR/NDcp were significantly higher than those of WKY and SHR/ND+ (Fig. 1b, c). Plasma insulin level and HOMA-IR of SHR/NDcp were strikingly higher than those of WKY and SHR/ND+ (Fig. 1h, i). Histopathological features of the H&E and ORO stained sections of livers from WKY, SHR/ND+ and SHR/NDcp are shown in Fig. 2a–f. In WKY, no vacuolation or lipid deposition was observed in hepatocytes, whereas several sinusoidal cells such as stellate cells were ORO-positive (Fig. 2a, b). Minimal to mild fat accumulation was seen in SHR/ND+ (Fig. 2c, d). In the case of SHR/NDcp, fat accumulation in hepatocytes was prominent. Diffuse macrovesicular fatty vacuolation and diffuse hepatocyte hypertrophy were seen (Fig. 2e, f). The intensity of fat accumulation in hepatocyte or hepatocyte hypertrophy of each animal was scored, as shown in Fig. 2g and h, respectively. There were no inflammatory changes such as hepatocellular necrosis, inflammatory cell

Fig. 2 Representative images showing the histology of liver sections from WKY (a, b), SHR/ND+ (c, d) and SHR/NDcp (e, f) stained with H&E (a, c, e) and ORO (b, d, f), and the intensity of fat accumulation in hepatocytes (g) and hypertrophy (h). Sections (e) and (f) show marked ORO-positive hepatocyte vacuolation. Scale bars indicate 200 and 500 μm in H&E- and ORO-stained sections, respectively. Insets show a higher magnification of the respective figure (b, d, f). The severity of histopathological findings was scored as (0) normal, (1) minimal, (2) mild, (3) moderate and (4) marked lipid deposition in hepatocytes



infiltration and fibrosis in the liver of SHR/NDcp. TAG contents in the liver of SHR/NDcp were 8.6-fold higher than those of WKY, but there was no significant difference in hepatic contents of TAG between WKY and SHR/ND+

(Fig. 1d). Notable differences were not observed in hepatic contents of either cholesterol or lipid phosphorus among the three groups of rats (Fig. 1e, f). There was no difference in the hepatic content of glycogen among WKY,

Table 2 Fatty acid composition of hepatic lipids (μmol or nmol/g liver)

	WKY ($\mu\text{mol/g}$ liver)	SHR/ND+ ($\mu\text{mol/g}$ liver)	SHR/NDcp ($\mu\text{mol/g}$ liver)
TAG			
16:0	5.41 \pm 0.75 ^a	4.85 \pm 1.07 ^a	55.11 \pm 22.46 ^b
16:1n-7	0.50 \pm 0.16 ^a	0.22 \pm 0.08 ^a	15.56 \pm 8.77 ^b
18:0	0.65 \pm 0.02 ^a	0.87 \pm 0.06 ^a	1.85 \pm 0.50 ^b
18:1n-9	3.86 \pm 0.41 ^a	3.09 \pm 1.02 ^a	49.74 \pm 24.36 ^b
18:1n-7	0.85 \pm 0.13 ^a	0.52 \pm 0.18 ^a	7.43 \pm 2.46 ^b
18:2n-6	6.20 \pm 1.06 ^a	4.75 \pm 1.78 ^a	27.07 \pm 14.74 ^b
18:3n-3	0.23 \pm 0.04 ^a	0.16 \pm 0.05 ^a	1.13 \pm 0.67 ^b
20:3n-9	0.07 \pm 0.01 ^a	0.07 \pm 0.01 ^a	0.13 \pm 0.03 ^b
20:3n-6	0.09 \pm 0.03 ^a	0.06 \pm 0.03 ^a	1.11 \pm 0.69 ^b
20:4n-6	0.63 \pm 0.17 ^{ab}	0.50 \pm 0.23 ^a	1.47 \pm 0.75 ^b
20:5n-3	0.34 \pm 0.06	0.12 \pm 0.06	0.89 \pm 0.65
22:5n-3	0.60 \pm 0.21 ^{ab}	0.24 \pm 0.14 ^a	1.54 \pm 1.00 ^b
22:6n-3	0.89 \pm 0.21	0.31 \pm 0.16	2.02 \pm 1.46
Total	20.31 \pm 3.06 ^a	15.74 \pm 4.76 ^a	165.04 \pm 77.95 ^b
DAG			
16:0	1.14 \pm 0.07 ^a	0.91 \pm 0.05 ^a	1.68 \pm 0.34 ^b
16:1n-7	0.14 \pm 0.02 ^a	0.08 \pm 0.01 ^a	0.62 \pm 0.14 ^b
18:0	0.65 \pm 0.11	0.51 \pm 0.04	0.51 \pm 0.08
18:1n-9	0.53 \pm 0.05 ^a	0.41 \pm 0.01 ^a	1.33 \pm 0.36 ^b
18:1n-7	0.37 \pm 0.03 ^{ab}	0.29 \pm 0.01 ^a	0.46 \pm 0.10 ^b
18:2n-6	2.44 \pm 0.24 ^a	2.07 \pm 0.03 ^{ab}	1.92 \pm 0.30 ^b
18:3n-3	0.03 \pm 0.00 ^a	0.02 \pm 0.00 ^b	0.04 \pm 0.01 ^a
20:3n-9	0.03 \pm 0.01	0.02 \pm 0.01	0.03 \pm 0.01
20:3n-6	0.05 \pm 0.00 ^a	0.03 \pm 0.00 ^b	0.16 \pm 0.02 ^c
20:4n-6	0.59 \pm 0.06 ^a	0.42 \pm 0.06 ^b	0.35 \pm 0.07 ^b
20:5n-3	0.04 \pm 0.00 ^a	0.02 \pm 0.00 ^b	0.03 \pm 0.00 ^c
22:5n-3	0.05 \pm 0.03	0.03 \pm 0.00	0.03 \pm 0.01
22:6n-3	0.09 \pm 0.01 ^a	0.05 \pm 0.00 ^b	0.05 \pm 0.01 ^b
Total	6.16 \pm 0.39 ^{ab}	4.86 \pm 0.18 ^a	7.21 \pm 1.28 ^b
	WKY (nmol/g liver)	SHR/ND+ (nmol/g liver)	SHR/NDcp (nmol/g liver)
CE			
16:0	356.4 \pm 41.5	311.5 \pm 22.0	384.8 \pm 58.0
16:1n-7	40.1 \pm 15.0 ^a	30.2 \pm 3.6 ^a	198.5 \pm 83.5 ^b
18:0	94.1 \pm 18.4	98.0 \pm 20.6	106.4 \pm 25.9
18:1n-9	152.4 \pm 33.8 ^a	133.0 \pm 20.0 ^a	347.9 \pm 137.1 ^b
18:1n-7	25.1 \pm 4.7 ^a	15.4 \pm 1.8 ^a	52.0 \pm 19.5 ^b
18:2n-6	144.0 \pm 28.1	128.6 \pm 18.0	174.4 \pm 62.7
18:3n-3	18.1 \pm 8.6	18.6 \pm 5.3	10.0 \pm 9.0
20:3n-9	29.1 \pm 4.9	30.4 \pm 3.6	32.2 \pm 2.2
20:3n-6	0.8 \pm 0.2 ^a	1.1 \pm 0.7 ^a	6.4 \pm 2.7 ^b
20:4n-6	78.1 \pm 12.7 ^a	59.6 \pm 16.1 ^a	129.3 \pm 34.9 ^b
20:5n-3	6.2 \pm 1.7 ^a	3.4 \pm 0.2 ^b	10.2 \pm 1.1 ^c
22:5n-3	2.8 \pm 1.3	1.9 \pm 1.6	3.6 \pm 0.5
22:6n-3	4.6 \pm 1.2 ^{ab}	2.3 \pm 1.9 ^a	6.9 \pm 2.2 ^b
Total	951.5 \pm 153.9 ^a	834.0 \pm 81.4 ^a	1,462.6 \pm 370.4 ^b

Table 2 continued

	WKY ($\mu\text{mol/g liver}$)	SHR/ND+ ($\mu\text{mol/g liver}$)	SHR/NDcp ($\mu\text{mol/g liver}$)
PL			
16:0	13.00 \pm 0.83	13.03 \pm 0.77	11.45 \pm 1.42
16:1n-7	0.42 \pm 0.11 ^a	0.25 \pm 0.02 ^a	1.28 \pm 0.19 ^b
18:0	12.03 \pm 0.53 ^a	12.03 \pm 0.40 ^a	10.00 \pm 0.34 ^b
18:1n-9	2.15 \pm 0.11	2.16 \pm 0.17	2.39 \pm 0.10
18:1n-7	2.93 \pm 0.21 ^a	2.03 \pm 0.16 ^b	2.10 \pm 0.47 ^b
18:2n-6	9.33 \pm 0.56 ^a	8.41 \pm 0.49 ^a	6.56 \pm 1.31 ^b
18:3n-3	0.07 \pm 0.01	0.09 \pm 0.08	0.03 \pm 0.01
20:3n-9	0.02 \pm 0.00	0.12 \pm 0.20	0.05 \pm 0.01
20:3n-6	0.40 \pm 0.03 ^a	0.31 \pm 0.02 ^a	1.85 \pm 0.33 ^b
20:4n-6	15.03 \pm 0.29 ^a	13.27 \pm 0.74 ^b	9.61 \pm 0.26 ^c
20:5n-3	0.41 \pm 0.12 ^a	0.11 \pm 0.01 ^b	0.32 \pm 0.10 ^a
22:5n-3	0.75 \pm 0.20	0.72 \pm 0.02	0.51 \pm 0.07
22:6n-3	2.94 \pm 0.32 ^a	3.74 \pm 0.35 ^b	2.97 \pm 0.33 ^a
Total	59.48 \pm 1.81 ^a	56.24 \pm 2.93 ^a	49.11 \pm 4.69 ^b

Values represent means \pm SD ($n = 4$). Differences in horizontal means without a common superscript (a, b, c) are significant ($p < 0.05$). In the absence of a superscript, the differences in the means are not significant ($p > 0.05$)

SHR/ND+ and SHR/NDcp (Fig. 1g). Prominent enrichment of 16:0, 18:1n-9, 16:1n-7 and 18:1n-7 was observed in hepatic TAG in SHR/NDcp; 18:2n-6 and 18:3n-3 were also enriched in TAG, but to a lesser extent than 16:0 and monounsaturated fatty acid (MUFA) (Table 2). On the other hand, no substantial enrichment of these fatty acids was found in PL, DAG or CE in the liver of SHR/NDcp.

Gene Expression

To gain insight into the molecular basis of TAG accumulation in the liver of SHR/NDcp, the mRNA levels of key enzymes and proteins involved in the metabolism of fatty acid and TAG in the liver were measured (Table 3). In the liver of SHR/NDcp, the levels of mRNAs encoding enzymes involved in *de novo* fatty acid synthesis [FAS, acetyl-CoA carboxylase 1 (ACC1), ATP-citrate lyase (ACLY) and malic enzyme 1 (ME1)], 18:1n-9 synthesis [Elovl6 and SCD1] and glycerolipid synthesis (GPAT1) were up-regulated, but that of ACSL1 was unchanged. There were no significant differences in the levels of mRNAs for DGAT1, DGAT2 and GPAT4 among WKY, SHR/ND+ and SHR/NDcp. With regard to proteins participating in the translocation and trafficking of fatty acids, the levels of mRNAs for fatty acid translocase (FAT/CD36) and ACSL5 in SHR/NDcp were significantly higher than those in WKY and SHR/ND+, respectively, whereas there were no significant differences in the levels of mRNAs encoding fatty acid transport protein (FATP)2, FATP4, FATP5, plasma membrane-associated fatty acid binding protein (FABPpm), fatty acid binding protein1 (FABP1) and ACSL1 between SHR/NDcp and SHR/ND+. The expression of the gene for ACSL3 was

significantly down-regulated in SHR/NDcp. The level of mRNA for L-type pyruvate kinase (LPK) in SHR/NDcp was 2.4-fold higher than those in WKY and SHR/ND+, and no considerable difference was found in the level of mRNA for phosphoenolpyruvate carboxykinase (PEPCK) between WKY and SHR/NDcp. The levels of mRNAs encoding enzymes involved in fatty acid degradation [carnitine palmitoyltransferase 1a (CPT1a), medium-chain acyl-CoA dehydrogenase (MCAD), and adipose triglyceride lipase (ATGL)] were significantly down-regulated in the liver of SHR/NDcp. On the other hand, no differences were found in the levels of mRNAs for long-chain acyl-CoA dehydrogenase (LCAD), very long-chain acyl-CoA dehydrogenase (VLCAD) and comparative gene identification-58 (CGI-58) between SHR/NDcp and WKY or SHR/ND+. As for nuclear transcription factors, the levels of SREBP-1c mRNA were 1.7- and 1.8-fold higher than those in WKY and SHR/ND+, respectively. On the one hand, there was no considerable difference in the gene expression of carbohydrate responsive element-binding protein (ChREBP), peroxisome proliferator-activated receptor α (PPAR α) or liver X receptor α (LXR α) between SHR/NDcp and SHR/ND+.

De Novo Fatty Acid Synthesis

The activities of cytosolic FAS, microsomal SCD, microsomal PCE and microsomal ACSL in the liver of SHR/NDcp were 7.7-, 5.0-, 4.0- and 1.3-fold, respectively, higher than those of WKY (Fig. 3a–d). The nuclear content of the mature 68-kDa form of SREBP-1c in the liver of SHR/NDcp was 6.4 and 9.1-fold higher than those of WKY and SHR/ND+, respectively (Fig. 4).

Table 3 Gene expressions in the liver

Genes	WKY	SHR/ND+	SHR/NDcp
Lipogenesis			
FAS	1.0 ± 0.19 ^a	0.58 ± 0.21 ^a	3.03 ± 0.81 ^b
ACC1	1.0 ± 0.13 ^a	0.79 ± 0.19 ^a	2.93 ± 0.55 ^b
ACLY	1.0 ± 0.11 ^a	0.60 ± 0.13 ^a	2.07 ± 0.75 ^b
ME1	1.0 ± 0.40 ^a	0.91 ± 0.36 ^a	1.62 ± 0.32 ^b
SCD1	1.0 ± 0.34 ^a	0.36 ± 0.28 ^b	5.27 ± 0.62 ^c
Elovl6	1.0 ± 0.35 ^a	1.07 ± 0.32 ^a	47.53 ± 19.61 ^b
DGAT1	1.0 ± 0.11	0.83 ± 0.10	0.85 ± 0.13
DGAT2	1.0 ± 0.21	0.82 ± 0.16	0.86 ± 0.08
GPAT1	1.0 ± 0.16 ^a	0.86 ± 0.18 ^a	1.40 ± 0.31 ^b
GPAT4	1.0 ± 0.20	1.05 ± 0.14	0.94 ± 0.08
Polyunsaturated fatty acid (PUFA) biosynthesis			
Fads1	1.0 ± 0.15 ^a	0.79 ± 0.19 ^b	0.15 ± 0.09 ^c
Fads2	1.0 ± 0.19 ^a	0.52 ± 0.25 ^b	0.53 ± 0.26 ^b
Elovl5	1.0 ± 0.31 ^a	0.71 ± 0.22 ^{ab}	0.63 ± 0.15 ^b
Fatty acid trafficking			
FAT/CD36	1.0 ± 0.66 ^a	0.15 ± 0.03 ^b	1.66 ± 0.40 ^c
FATP2	1.0 ± 0.20 ^a	0.87 ± 0.14 ^{ab}	0.73 ± 0.11 ^b
FATP4	1.0 ± 0.34	1.16 ± 0.60	0.70 ± 0.18
FATP5	1.0 ± 0.35 ^a	0.75 ± 0.21 ^{ab}	0.58 ± 0.17 ^b
FABPpm	1.0 ± 0.14 ^a	0.91 ± 0.06 ^{ab}	0.83 ± 0.12 ^b
FABP1	1.0 ± 0.24 ^a	0.76 ± 0.14 ^b	0.70 ± 0.12 ^b
ACSL1	1.0 ± 0.17	0.93 ± 0.11	0.97 ± 0.11
ACSL3	1.0 ± 0.15 ^a	1.37 ± 0.25 ^b	0.44 ± 0.11 ^c
ACSL5	1.0 ± 0.11 ^a	0.56 ± 0.17 ^b	1.72 ± 0.03 ^c
Lipid degradation			
CPT1a	1.0 ± 0.38 ^a	1.15 ± 0.13 ^a	0.45 ± 0.06 ^b
MCAD	1.0 ± 0.19 ^a	1.06 ± 0.17 ^a	0.72 ± 0.04 ^b
LCAD	1.0 ± 0.13	1.04 ± 0.20	1.17 ± 0.15
VLCAD	1.0 ± 0.18	0.95 ± 0.17	0.85 ± 0.08
ATGL	1.0 ± 0.20 ^a	1.09 ± 0.20 ^a	0.61 ± 0.11 ^b
CGI-58	1.0 ± 0.41	0.59 ± 0.16	0.64 ± 0.11
Glucose metabolism			
LPK	1.0 ± 0.25 ^a	1.02 ± 0.33 ^a	2.39 ± 0.46 ^b
PEPCK	1.0 ± 0.16 ^{ab}	1.07 ± 0.14 ^a	0.81 ± 0.14 ^b
Nuclear transcription factors			
SREBP-1c	1.0 ± 0.29 ^a	0.93 ± 0.11 ^a	1.71 ± 0.36 ^b
ChREBP	1.0 ± 0.43 ^a	0.67 ± 0.25 ^{ab}	0.45 ± 0.05 ^b
PPAR α	1.0 ± 0.36	0.72 ± 0.21	0.73 ± 0.17
LXR α	1.0 ± 0.26 ^a	0.75 ± 0.10 ^{ab}	0.67 ± 0.15 ^b

Values represent means \pm SD ($n = 4-8$). Differences in horizontal means without a common superscript (a, b, c) are significant ($p < 0.05$). In the absence of a superscript, the differences in the means are not significant ($P > 0.05$)

TAG Synthesis

Incorporations of [¹⁴C]18:1n-9 into TAG, DAG, CE and PL in the liver of WKY, SHR/ND+ and SHR/NDcp were

compared *ex vivo* using liver slices (Fig. 5). The incorporation of radio-labeled 18:1n-9 into TAG in the liver slices of SHR/NDcp was 1.5 and 1.6-fold greater than those of WKY and SHR/ND+, respectively (Fig. 5a). There were no considerable differences in the incorporation of [¹⁴C]18:1n-9 into DAG, CE or PL among the three groups of rats (Fig. 5b–d). The concentration of unesterified 18:1n-9 in the liver of SHR/NDcp was 1.9 and 1.7-fold higher than those of WKY and SHR/ND+, respectively (Table 4). It is, therefore, reasonable to assume that the absolute amount of 18:1n-9 incorporated into TAG in the liver slices of SHR/NDcp is much greater than that calculated on the basis of incorporated radioactivity. On the other hand, there was no significant difference in the activity of microsomal GPAT among WKY, SHR/ND+ and SHR/NDcp (Fig. 3e). Moreover, the activity of microsomal DGAT in the liver of SHR/NDcp was 73 % of that of WKY, but no significant difference was observed in the activity between SHR/NDcp and SHR/ND+ (Fig. 3f).

Fatty Acid Oxidation

To confirm the functional significance of the reduced expression of the genes of ATGL, CPT1a and MCAD, rates of [¹⁴C]16:0 oxidation in the liver of WKY, SHR/ND+ and SHR/NDcp were compared *ex vivo* using liver slices (Fig. 6). The rates of formation of both CO₂ and acid soluble oxidation products in liver slices of SHR/NDcp were strikingly lower than those of WKY and SHR/ND+ (Fig. 6b, c). No significant difference was observed in the rate of [¹⁴C]16:0 oxidation between WKY and SHR/ND+ (Fig. 6a). It is worth noting that there was no significant difference in the concentrations of unesterified 16:0 in the livers among WKY, SHR/ND+ and SHR/NDcp (Table 4).

PUFA Synthesis

The content of 20:3n-6 in PL in the liver of SHR/NDcp was markedly higher than those of WKY and SHR/ND+; conversely, the content of 20:4n-6 in PL in the liver of SHR/NDcp was considerably lower than those of WKY and SHR/ND+ (Table 2). Levels of mRNA encoding Fads1 were 15 and 19 %, respectively, of those of WKY and SHR/ND+ (Table 3). On the other hand, there were no significant differences in mRNA levels of Fads2 and Elovl5 between SHR/NDcp and SHR/ND+, whereas those of SHR/NDcp were significantly lower than those of WKY.

ER Stress

To explore whether perturbation of lipid metabolism in the liver causes ER stress in SHR/NDcp, the PtdCho/PtdEtn ratio in microsomal lipid and the expression patterns of

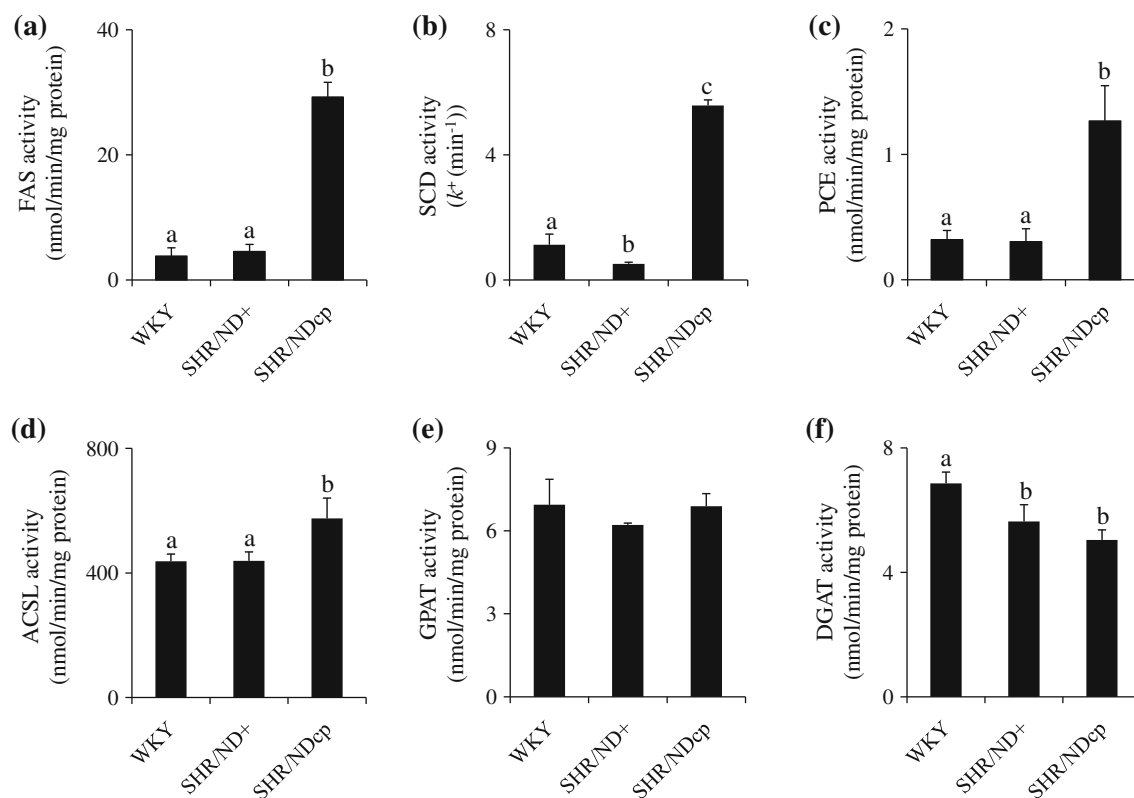


Fig. 3 Activities of enzymes involved in lipogenesis. **a** FAS in cytosol, **b** SCD in microsomes, **c** PCE in microsomes, **d** ACSL in microsomes, **e** GPAT in microsomes, **f** DGAT in microsomes. Values

represent mean \pm SD ($n = 4$). ^{a, b, c} Differences without a common superscript are statistically significant ($p < 0.05$). In the absence of a superscript, the differences in the means are not significant ($p > 0.05$)

several molecular indicators of ER stress were estimated (Fig. 7). The PtdCho/PtdEtn ratio in microsomal lipid in the liver of SHR/NDcp was 1.13 and 1.36-fold higher than those of WKY and SHR/ND+, respectively (Fig. 7a). Figure 7b shows the differences in the proportions (mol%) of fatty acids in microsomal PtdCho and PtdEtn between SHR/NDcp and WKY and between SHR/ND+ and WKY. In PtdCho of SHR/NDcp, the proportions of MUFA and 20:3n-6 were increased and, conversely, that of 20:4n-6 was decreased. The extents of the changes in PtdEtn of SHR/NDcp were not as great as those observed in PtdCho. No significant differences were observed in the expression of mRNAs encoding glucose-regulated protein 78 kDa (GRP78), CCAAT/enhancer binding protein homologous protein (CHOP) and XBP1 among WKY, SHR/ND+ and SHR/NDcp (Fig. 7c–e). Moreover, an increase in splicing of XBP1 mRNA was not observed in the liver of SHR/NDcp (Fig. 7f).

Discussion

The present study showed that deposition of TAG, but neither cholesterol nor PL, in hepatocytes was strikingly

accelerated in SHR/NDcp in comparison with those in WKY and SHR/ND+. The current data revealed that the TAG content in the liver of SHR/NDcp was approximately 5 % by weight. Moreover, histopathological analyses demonstrated the presence of lipid droplets in hepatocytes of SHR/NDcp. However, inflammatory changes such as hepatocellular necrosis, inflammatory cell infiltration and fibrosis were not observed in the liver of SHR/NDcp. Therefore, the liver conditions in SHR/NDcp are largely considered to involve simple steatosis. Our previous study showed that a marked increase in the hepatic content of particular fatty acid species, 16:0, 16:1n-7, 18:1n-9, 18:1n-7 and 20:3n-6, is characteristic of SHR/NDcp in comparison with WKY, SHR, SHRSP and SHR/ND+ [12]. The present study confirmed that, in SHR/NDcp, the increased TAG was enriched with these fatty acid species, in particular 16:0 and 18:1n-9.

Since fatty liver disease *per se* is linked to insulin resistance and thus by itself may be a major aggravating factor in the pathogenesis and progression of MS and its associated disorders [31], it is important to elucidate mechanism contributing to TAG accumulation in the liver of SHR/NDcp. Irrespective of the origin of FFA, increased hepatic lipid supply most probably contributes to hepatic

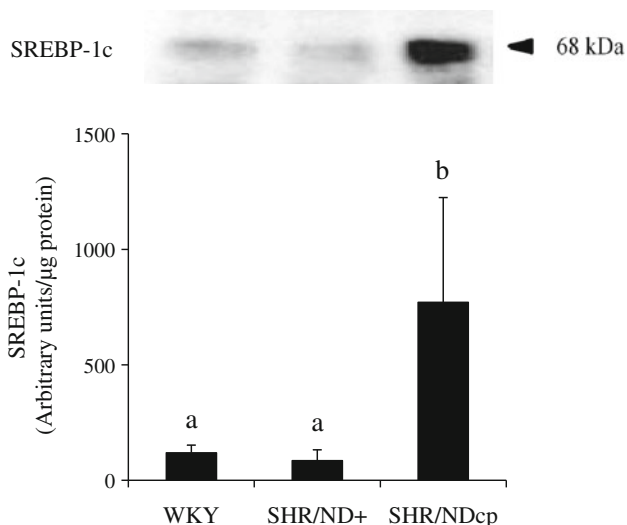
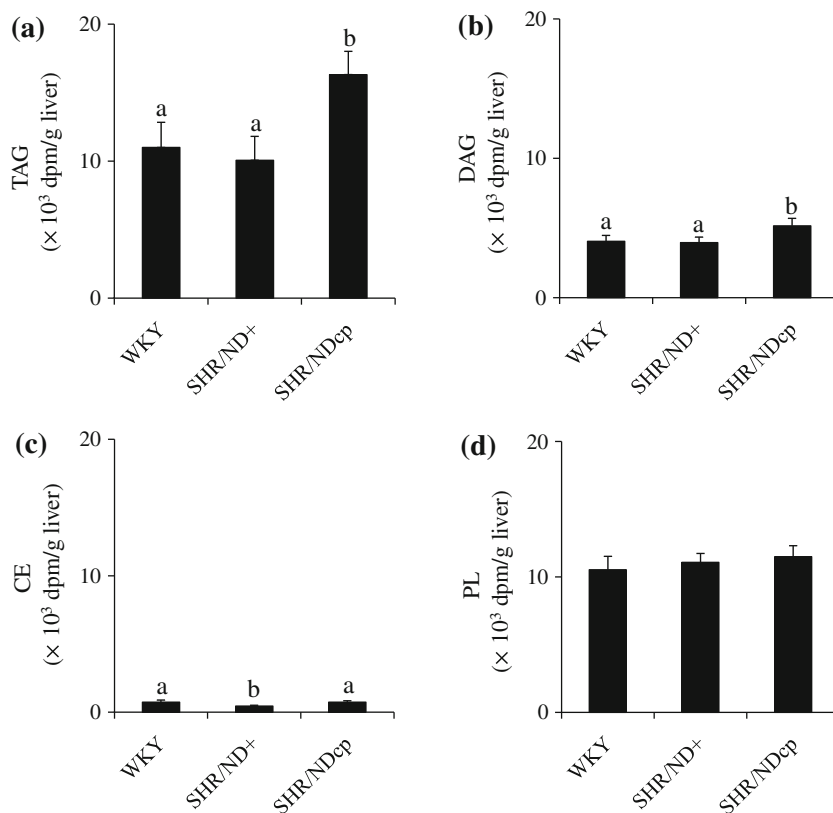


Fig. 4 Protein expression of mature form of SREBP-1c in nuclear extracts from livers. Immunoblots were carried out on nuclear extracts from livers. Nuclear extracts of WKY (20 μ g of protein), SHR/ND+ (30 μ g of protein) and SHR/NDcp (7.5 μ g of protein) were loaded and separated by electrophoresis. Visible bands are SREBP-1c as indicated. Quantification for the amount of SREBP-1c was carried out using Multi gauge software (GE Healthcare) and normalized by loaded protein content. Values represent means \pm SD ($n = 3-4$). ^{a, b} Differences without a common superscript are statistically significant ($p < 0.05$)

Fig. 5 Incorporation *ex vivo* of [¹⁴C]18:1n-9 into lipids in liver slices. Liver slices were incubated with 0.25 mM [1-¹⁴C]18:1n-9 for 10 min at 37 $^{\circ}$ C. The lipids were extracted from liver slices and separated by TLC. **a** TAG, **b** DAG, **c** CE, **d** PL. Values represent mean \pm SD ($n = 4$). ^{a, b} Differences without a common superscript are statistically significant ($p < 0.05$). In the absence of a superscript, the differences in the means are not significant ($p > 0.05$)



TAG accumulation [32]. Namely, hepatic lipid accumulation may result from an imbalance between lipid availability and lipid disposal; the excessive TAG deposition in the liver could be initiated by (1) increased *de novo* synthesis of fatty acid, (2) increased delivery of fatty acid from extra hepatic sources, (3) increased TAG synthesis, (4) decreased β -oxidation of fatty acid, and (5) decreased secretion of very low density lipoprotein, or several of these factors in combination. To deal with these possibilities, the approaches that we employed in the present study are as follows: first, to decide the targets on which the present study focuses, the expression of genes encoding enzymes and proteins for lipogenesis, fatty acid translocation/trafficking, fatty acid degradation, and nuclear transcription factors for the regulation of lipid metabolism was measured; second, the activities of enzymes and levels of proteins selected as targets in our study were determined; and third, TAG formation and fatty acid degradation were estimated *ex vivo* using precision-cut liver slices.

As for *de novo* fatty acid synthesis, the activity of FAS in SHR/NDcp was strikingly higher than those in WKY and SHR/ND+, which is consistent with the higher expression of the mRNA for FAS in SHR/NDcp. The elevated expression of genes for ACC1, ACLY and ME1 in

Table 4 FFA in the liver (nmol/g liver)

	WKY	SHR/ND+	SHR/NDcp
16:0	327.54 ± 51.30	350.34 ± 97.22	355.69 ± 50.47
16:1n-7	5.52 ± 2.84 ^a	4.56 ± 1.00 ^a	20.35 ± 5.06 ^b
18:0	68.98 ± 10.60	75.74 ± 13.41	74.42 ± 10.37
18:1n-9	37.62 ± 8.17 ^a	41.31 ± 8.36 ^a	70.50 ± 8.66 ^b
18:1n-7	15.90 ± 5.36	10.97 ± 3.57	16.37 ± 2.94
18:2n-6	39.05 ± 12.65	40.70 ± 12.15	32.80 ± 6.80
18:3n-3	12.27 ± 8.41	11.12 ± 2.01	19.32 ± 6.10
20:3n-9	6.92 ± 7.79	2.80 ± 2.09	12.56 ± 4.00
20:3n-6	0.43 ± 0.34 ^{ab}	0.32 ± 0.09 ^a	1.49 ± 0.89 ^b
20:4n-6	21.25 ± 6.76	17.18 ± 5.51	16.00 ± 3.45
20:5n-3	2.39 ± 0.97 ^{ab}	1.30 ± 0.39 ^a	4.22 ± 2.03 ^b
22:5n-3	2.73 ± 1.94	2.88 ± 0.68	2.50 ± 1.08
22:6n-3	5.55 ± 3.81	6.25 ± 3.53	5.98 ± 1.88
Total	546.16 ± 83.61	565.47 ± 140.34	632.17 ± 84.35

Values represent means ± SD ($n = 4$). Differences in horizontal means without a common superscript (a, b) are significant ($p < 0.05$). In the absence of a superscript, the differences in the means are not significant ($p > 0.05$)

the liver of SHR/NDcp strongly suggests the stimulated supplies of both malonyl-CoA and NADPH for FAS. Moreover, the increased gene expression of LPK suggests that the supply of acetyl-CoA from glucose is also increased in hepatocytes of SHR/NDcp. These results, taken together, strongly imply the increased formation of 16:0 in the liver of SHR/NDcp, a suggestion that is consistent with the previous finding that the liver of SHR/NDcp contains 16:0 in large quantities [12]. Moreover, the 16:0 produced by FAS may be converted to palmitoyl-CoA by microsomal ACSL, the activity of which in the liver of SHR/NDcp was higher. Considering the ratios of 16:0/18:2n-6 and 18:1n-9/18:2n-6 (0.55 and 0.47, respectively) in the chow diet on which rats were fed in the present

study, the corresponding ratios of fatty acids in TAG in SHR/NDcp were markedly higher than those in WKY (16:0/18:2n-6 = 2.14 *versus* 0.88; 18:1n-9/18:2n-6 = 1.86 *versus* 0.63). These results suggest that the not small fraction of palmitoyl-CoA that was increasingly supplied was elongated by PCE (encoded by Elov16) and then de-saturated by SCD (encoded by SCD1) to oleoyl-CoA and that palmitoyl-CoA and oleoyl-CoA produced by *de novo* fatty acid synthesis were utilized to form TAG. Similarly, the increased formations of palmitoleoyl-CoA and *cis*-vaccenoyl-CoA were likely to occur concurrently with the elevated formation of oleoyl-CoA. Activation of nuclear transcription factors, such as SREBP-1c, ChREBP and LXR α , is considered to contribute to the synthesis of 16:0 and 18:1n-9 through the up-regulation of FAS, SCD1 and Elov16 [33, 34], and the increased *de novo* lipogenesis is secondary to the augmented expression of both SREBP-1c and ChREBP in insulin resistance and type 2 diabetes [35, 36]. The present study showed that the gene expression of SREBP-1c, but not ChREBP or LXR α , was significantly elevated in the liver of SHR/NDcp and that the nuclear content of the mature form of SREBP-1c in the liver of SHR/NDcp was markedly higher than those of WKY and SHR/ND+. These results are consistent with the findings that, in animal models, insulin has been shown to stimulate lipogenesis through SREBP-1c, even in insulin-resistant liver [37]. Shimomura et al. [38] have demonstrated that, despite the profound hepatic insulin resistance concerning glucose production through down-regulation of insulin-receptor-substrate-2, insulin continues to stimulate the production of SREBP-1c in the liver of insulin-resistant and hyperinsulinemic *ob/ob* mice. The present study showed that SHR/NDcp also exhibited evident insulin resistance and hyperinsulinemia, results that are in accordance with previously reported findings [6, 7]. These findings, taken together, prompt one to speculate that

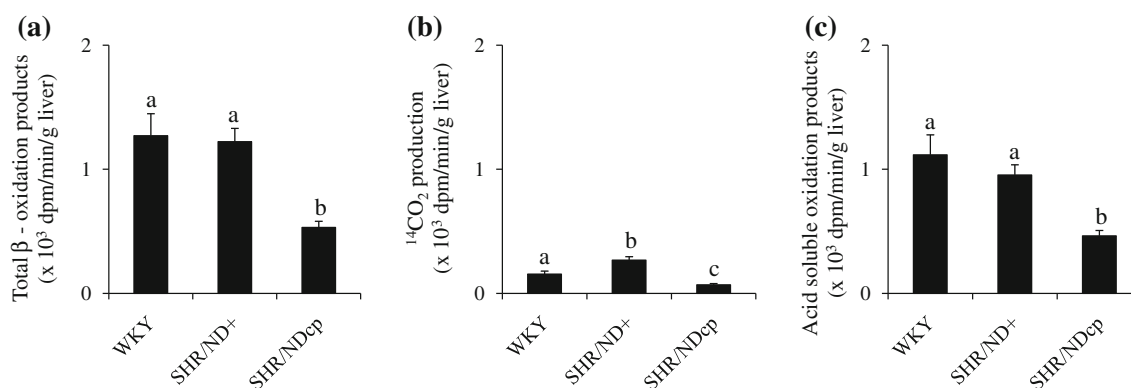
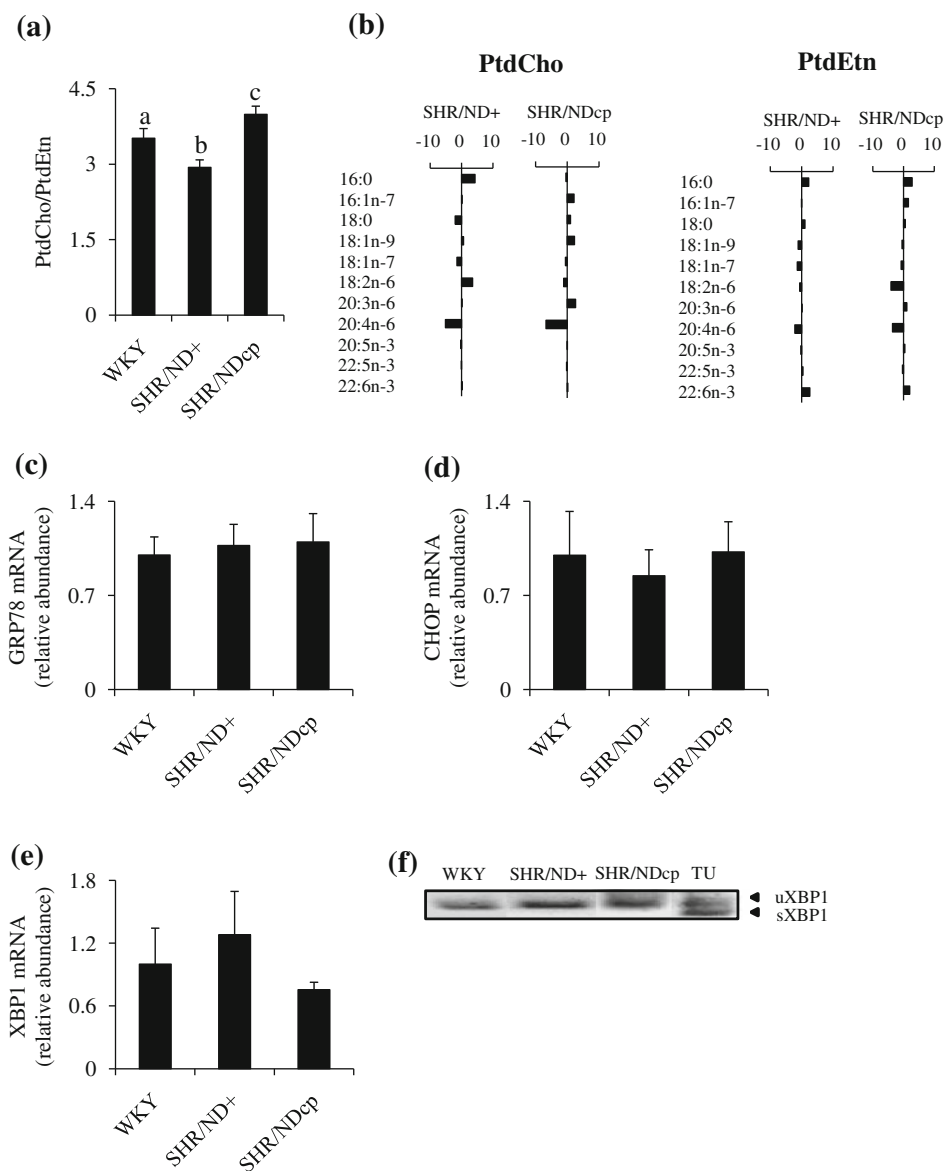


Fig. 6 Oxidation *ex vivo* of [^{14}C]16:0 in liver slices. Liver slices were incubated with 0.25 mM [^{14}C]16:0 for 30 min at 37 °C. The $^{14}\text{CO}_2$ produced was trapped with benzethonium hydroxide, and acid soluble oxidation products were extracted. **a** Total β -oxidation

products, **b** CO_2 , **c** Acid soluble oxidation products. Values represent means ± SD ($n = 4$). a, b, c Differences without a common superscript are statistically significant ($p < 0.05$)

Fig. 7 PL composition in microsomes and expressions of ER stress responsive genes in the liver. **a** Relative abundance of PtdCho and PtdEtn in hepatic microsomes, **b** differences in proportion (mol%) of each fatty acid in PtdCho and PtdEtn of microsomes between the means of SHR/ND+ and WKY and between the means of SHR/NDcp and WKY. Microsomal lipids were extracted and microsomal PL were separated by TLC, and fatty acids in individual PL were determined by gas chromatography. Relative gene expressions of **c** GRP78, **d** CHOP, **e** XBP1, and **f** unspliced XBP1 (uXBP1) and spliced XBP1 (sXBP1). In **f**, TU represents the results of the following experiments: McA-RH7777 cells were incubated for 3 h in Dulbecco's modified Eagle's medium supplemented with 10 μ g/mL tunicamycin, and uXBP1 and sXBP1 were measured by PCR followed by electrophoresis. Values represent means \pm SD ($n = 4-8$). ^{a, b, c} Differences without a common superscript are statistically significant ($p < 0.05$). In the absence of a superscript, the differences in the means are not significant ($p > 0.05$)



SREBP-1c transcription and protein expression are enhanced in the liver of SHR/NDcp by insulin action that is mediated through the insulin-receptor-substrate-1-dependent pathway. Moreover, the present results suggest that hyperinsulinemia plays a pivotal role in the up-regulation of lipogenic enzymes, FAS, ACC1, ACLY, ME1, SCD1 and Elovl6, in the liver of SHR/NDcp.

The present study showed that formation of [14 C]TAG from [14 C]18:1n-9 in liver slices of SHR/NDcp was 1.5-fold higher than that of WKY, indicating that the rate of incorporation of 18:1n-9, which is delivered from the circulation, into TAG is up-regulated in the liver of SHR/NDcp in comparison with those in WKY and SHR/ND+. It should be noted here that it is impossible to calculate the absolute amounts of 18:1n-9 incorporated into TAG from these data, because [14 C]18:1n-9 entered hepatocytes in the

liver slices from the incubation medium and then mixed with endogenous unesterified 18:1n-9, which already exists in 18:1n-9 pools in hepatocytes, before being utilized for TAG synthesis. However, little information is available as to the number and size of 18:1n-9 pools in the liver. In the present study, therefore, the absolute amount of 18:1n-9 incorporated into TAG was not calculated, and the results are presented as the values of radioactivity in TAG. Since the hepatic concentration of 18:1n-9 in SHR/NDcp was 1.9-fold greater than that in WKY, the radiospecific activity of [14 C]18:1n-9 that entered hepatocytes in the liver slices may be reduced by endogenous unesterified 18:1n-9 in SHR/NDcp to 1/1.9 of that of WKY. As a result, the absolute amount of TAG that was formed by incorporation of 18:1n-9 in the liver of SHR/NDcp is assumed to be roughly 2.9-fold greater than that of WKY. However,

the detailed role of hepatic pools of unesterified 18:1n-9 remains controversial. There are two sources of fatty acids as substrates for TAG synthesis. One is the fatty acids taken up from the circulation, and the other is the fatty acids synthesized *de novo* in the liver. FAT/CD36 plays a central role in the uptake of circulating FFA into hepatocytes [39]. The present study showed that the expression of the gene encoding FAT/CD36 in SHR/NDcp was 1.7- and 11-fold higher than those in WKY and SHR/ND+, respectively, and that the activity of microsomal ACSL was up-regulated in the liver of SHR/NDcp in association with the enhanced expression of the gene for ACSL5. Therefore, in the liver of SHR/NDcp, fatty acids as substrates for the synthesis of intrahepatic TAG may be increasingly supplied. It has been shown that increased FFA delivery to the liver stimulates the synthesis of TAG in hepatocytes [32, 40]. Moreover, on the basis of the current results, it is most likely that the supplies of 16:0 and MUFA, in particular 18:1n-9, that are synthesized *de novo* are augmented. Nevertheless, little evidence is available as to the proportions of fatty acids in terms of their origin, namely, the circulation and/or *de novo* synthesis within hepatocytes, for TAG synthesis. It is known that 11 % of hepatic TAG is derived from *de novo* lipogenesis in rats that are healthy and are fed on a chow diet [41]. On the one hand, the contribution of *de novo* fatty acid synthesis to intrahepatic TAG may be greater in SHR/NDcp, because it has been reported that 26 % of TAG arises from *de novo* lipogenesis while serum FFA account for up to 60 % of hepatic TAG in patients with nonalcoholic fatty liver disease (NAFLD) [42]. Collectively, even in the setting of hepatic over-accumulation of TAG, the contribution of *de novo* fatty acid synthesis in SHR/NDcp may be less than that of fatty acids derived from peripheral tissues or dietary fat. With respect to PUFA, the contents of 18:2n-6 and 18:3n-3 in hepatic TAG of SHR/NDcp were considerably higher than those of WKY and SHR/ND+, increases that are probably due to augmented uptake of these fatty acids from the circulation by the up-regulated FAT/CD36.

As for the enzymes that contribute to TAG synthesis, the present study revealed that there was no up-regulation of activities of GPAT and DGAT in microsomes of the liver of SHR/NDcp, the results that were consistent with the expression of genes for GPAT4, DGAT1 and DGAT2. Thus, there is an apparent discrepancy between the increased incorporation of [¹⁴C]18:1n-9 into TAG and the activities of the enzymes for TAG synthesis. However, similar findings were reported by Jamdar and Cao [43], who showed no differences in the microsomal activities of GPAT and DGAT between lean and obese Zucker rats, despite the hepatic content of TAG in obese Zucker rats being much greater than that in lean control. GPAT catalyzes the first, rate-limiting step in glycerolipid synthesis

[44]. In the liver, GPAT 4 resides in the ER, and GPAT1 is localized in the outer mitochondrial membrane [44]. Although GPAT1 is a mitochondrial isoform and DGAT resides in the ER, many studies support the important role for GPAT1 in regulating TAG synthesis in the liver [45]. The present study showed that the expression of the gene for GPAT1 in the liver of SHR/NDcp was higher than those in controls (WKY and SHR/ND+). This increased expression of GPAT1 mRNA in the liver of SHR/NDcp is reasonable because GPAT1 has been demonstrated to be regulated by insulin through SREBP-1c, but neither LXR nor ChREBP [46]. DGAT2 appears to play a dominant role in the liver [47]. The present study revealed that no difference was found in the gene expression of either DGAT1 or DGAT2 between SHR/NDcp and controls. However, 18:1n-9, which is increasingly taken up by FAT/CD36, may be converted to oleoyl-CoA by ACSL5 with elevated activity and the oleoyl-CoA is likely to be utilized as a substrate for DGAT in the ER. The strikingly elevated *de novo* formation of 18:1n-9 in the liver of SHR/NDcp may also supply a massive amount of substrate for DGAT2, because SCD1 has been shown to co-localize with DGAT2 in the ER [48] and is considered to impact the rate of glycerolipid synthesis [49, 50]. Collectively, the existing evidence suggests that the oversupply of substrates (16:0 and 18:1n-9), derived from the circulation and from *de novo* synthesis, for both GPAT and DGAT is a major cause of the increased formation of TAG in the liver of SHR/NDcp.

It is considered that dysregulated mitochondrial metabolism of fatty acids is central in fatty liver [51]. The current data revealed that the rate of 16:0 β -oxidation in liver slices of SHR/NDcp was substantially lower than those of WKY and SHR/ND+, with the value being 42 % of that of WKY. These results are consistent with the decreased expression of genes encoding CPT1a and MCAD. CPT1a is considered to catalyze the rate-limiting step in β -oxidation and to play a pivotal role in controlling TAG content in the liver [52]. ATGL is a key enzyme that is responsible for hydrolyzing the first fatty acid from TAG and deficiency of ATGL is known to cause progressive hepatic steatosis [53]. Thus, in addition to the increased *de novo* lipogenesis, the impairment of ATGL and mitochondrial β -oxidation is likely to increase automatically the availability of fatty acids for TAG synthesis, which seems to be causative of TAG accumulation in the liver of SHR/NDcp.

The profiles of 20:3n-6, 20:4n-6, 20:5n-3 and 22:6n-3 are known to influence the levels of pro-inflammatory and anti-inflammatory products, such as different series of prostanoids, different series of leukotrienes, lipoxins and resolvins. The present study revealed that the profile of PUFA in hepatic lipids, in particular PL, was considerably perturbed in SHR/NDcp. In hepatic PL in SHR/NDcp,

20:3n-6 was markedly enriched and the content of 20:4n-6 was significantly lower than that of controls. 20:4n-6 is known to be formed from 18:2n-6. Namely, 18:2n-6 is desaturated by $\Delta 6$ desaturase (encoded by *Fads2*) to 18:3n-6. This is followed by an elongation step mediated by fatty acid elongase (encoded by *Elovl5*) to 20:3n-6, after which $\Delta 5$ desaturase (encoded by *Fads1*) forms 20:4n-6. The alterations in PUFA proportion that were brought about in the liver of SHR/NDcp may be elucidated by the facts that the expression of *Fads1* was strikingly down-regulated and that, on the other hand, there were no significant differences in the expression of *Fads2* and *Elovl5* between SHR/NDcp and SHR/ND+. The expression pattern of *Fads1*, *Fads2* and *Elovl5* in the liver of SHR/NDcp is very similar to that of Zucker *falfa* rats [23]. These three genes are considered to share common regulatory characteristics including regulation by SREBP-1c and PPAR α [33], regulation that is similar to those of *SCD1* and *Elovl6* [33]; the present results also demonstrated the increased nuclear content of the mature form of SREBP-1c and the marked up-regulation of *SCD1* and *Elovl6*. However, the mechanism responsible for differential regulation of the expression of these three genes (*Fads1*, *Fads2* and *Elovl5*) in the liver of SHR/NDcp remains to be demonstrated. The present results showed that, different from 20:4n-6, the contents of 20:5n-3 and 22:6n-3, the biosynthetic pathway of which also involves $\Delta 5$ desaturase, were little changed in the liver of SHR/NDcp. Although the mechanism behind the phenomenon that the formation of 20:4n-6 was reduced while biosynthesis of 20:5n-3 and 22:6n-3 was not affected remains unresolved, it is noteworthy that the chow on which the rats were fed contained higher proportions of 20:5n-3 (2.9 %) and 22:6n-3 (1.3 %) than of 20:4n-6 (0.2 %). Further study is required to understand whether an imbalance in PUFA in the liver leads to induction or progression of metabolic-inflammatory pathologies in SHR/NDcp.

Increased FFA and TAG contents in hepatocytes in insulin resistance have been demonstrated to prompt ER stress [54]. Disturbance of fatty acid species composition, in particular overaccumulation of saturated fatty acids (SFA), and phospholipid composition are starting to be considered as causes of hepatic ER stress [9, 10, 55]. Recently, it has been demonstrated that increased *de novo* fatty acid synthesis in the liver of *ob/ob* mice produces ample amounts of MUFA, which is effectively incorporated into PtdCho but not PtdEtn, which further distorts the PtdCho/PtdEtn ratio and impairs ER function [55]. Moreover, the increase in SREBP-1c expression and the resulting elevation of lipogenesis in the liver could be related to augmented ER stress in insulin resistance and type 2 diabetes [56, 57]. As for SHR/NDcp, the present study showed the increased *de novo* synthesis of 16:0 and 18:1n-9, the

accumulation of TAG containing 16:0 and 18:1n-9 with high proportions, lipid droplets and a slightly but significantly higher PtdCho/PtdEtn ratio in ER in the liver. Moreover, SHR/NDcp exhibit insulin resistance and type 2 diabetes. These facts, taken together, might imply that SHR/NDcp are under hepatic ER stress. The present study confirmed, however, that there were no differences in the mRNA levels of GPR78, CHOP and s-XBP1 in the liver among WKY, SHR/ND+ and SHR/NDcp.

The major findings of the present study are that SHR/NDcp exhibit (1) hepatic simple steatosis (fat accumulation as lipid droplets), (2) accumulation of TAG containing 16:0, 18:1n-9 and 16:1n-7 in high proportions, (3) up-regulation of *de novo* fatty acid synthesis (*FAS*, *SCD1* and *Elovl6*), (4) up-regulation of TAG synthesis and (5) down-regulation of TAG degradation (*ATGL*, fatty acid β -oxidation). Numerous studies have suggested, using different kinds of experimental models, that *SCD1* plays a central role in TAG accumulation. A typical example of this is a study using Zucker *falfa* rats, a model of MS; pharmacologic inhibition of *SCD* has been revealed to decrease the levels of TAG in the liver and to improve glucose tolerance [58]. Thus, it seems possible that *SCD1* is one of the major contributors to MS. On the other hand, compared with *SCD1*, little is known about *Elovl6* in relation to MS. However, there is suggestive evidence indicating a close relationship between *Elovl6* and *SCD1* with regard to disorder of lipid metabolism in the liver. The expression of the *Elovl6* gene in liver-specific *SCD1* knockout mice is not up-regulated in response to feeding on a high-carbohydrate diet, despite the fact that expression of the gene is inducible in normal liver [50]; conversely, in the liver of *Elovl6* knockout mice, expression of the *SCD1* gene is also down-regulated and the mice exhibit amelioration of insulin resistance [59]. More recently, we have revealed that *SCD1* is markedly up-regulated, while the level of *Elovl6* remains unchanged in the liver of Goto-Kakizaki rats, which exhibit type 2 diabetes without obesity, and that the content and proportion of 18:1n-9 in hepatic lipids of the rats are little changed [23]. These findings may imply that up-regulation of *Elovl6* in conjunction with *SCD1* is necessary for the increased formation of 18:1n-9. In contrast to other animal models [60], notable ER stress was not detected in the liver of SHR/NDcp. Previous studies on cultured cells have revealed that one can ward off the lipotoxic effects of SFA by supplementation with MUFA such as 18:1n-9, which promotes the incorporation of the SFA into the TAG pool [11, 61, 62]. Namely, it is suggested that an increased saturated FFA/unsaturated FFA ratio in the liver triggers lipotoxicity and that this condition ensues when the hepatic capacity to remove saturated FFA is overwhelmed. Saturated FFA are not readily esterified by hepatocytes, conversion of SFA to MUFA, in particular

18:1n-9, being necessary for easier incorporation into TAG. Therefore, it is most likely that, owing to the marked up-regulation of SCD1 and Elovl6, hepatocytes of SHR/NDcp successfully evaded elevation of ER stress by partitioning excess SFA independently of their origin (exogenous or *de novo* synthesized) into MUFA that can be safely stored as TAG, an inert storage lipid. Thus, SCD1 in conjunction with Elovl6 may not only cause hepatic steatosis, but also make important contributions to prevent the progression of simple steatosis to severe steatosis or steatohepatitis as a molecular switch towards esterification of FFA to TAG in hepatocytes, which may protect the liver from lipotoxicity by buffering the accumulation of FFA, in particular SFA. The findings obtained in the present study may further support the pathophysiological role of SCD1 and Elovl6 in the liver of MS.

Although there is growing evidence, not much is known with respect to fatty acid metabolism in the liver of humans in MS. NAFLD, namely TAG accumulation in the liver, is considered to be a feature of MS in humans [8]. Importantly, it has been confirmed, by human study, that the hepatic expression of SREBP-1c is markedly greater in the liver in NAFLD than in controls and that the expression of insulin-receptor-substrate-1 positively correlates with SREBP-1c [63]. It is known that hepatic lipogenesis, estimated *in vivo*, is increased in the liver of human subjects with obesity and hyperinsulinemia [64]. Hepatic SCD activity, which is estimated as 18:1n-9/18:0 or 16:1n-7/16:0 ratio in serum lipids, is also elevated in humans in MS [65, 66]. Hepatic $\Delta 5$ desaturase is down-regulated, whereas the role of $\Delta 6$ desaturase in the liver of humans in MS or NAFLD remains controversial [65–67]. The fatty acid profile has been characterized as having higher proportions of 16:1n-7, 18:1n-9 and 20:3n-6 in serum lipids [65, 67] and lower proportions of 18:2n-6 and 20:4n-6 in hepatic PL [68] in MS or NAFLD. To our knowledge, whether fatty acid elongases (Elovl6 and Elovl5) and fatty acid β -oxidation play central roles in the pathogenesis of MS or NAFLD in humans remains unclear. Thus, the current results regarding disorders of fatty acid metabolism in the liver of SHR/NDcp are very similar to those reported in the liver of human subjects in MS. Therefore, SHR/NDcp is most likely to be a useful model of human MS with hepatic simple steatosis.

Acknowledgments We thank Chiho Kojiguchi for her very helpful technical assistance. This work was supported by a Grant-in-Aid for Scientific Research from the Ministry of Education, Culture, Sports, Science and Technology of Japan.

References

- Koletsky S (1975) Pathologic findings and laboratory data in a new strain of obese hypertensive rats. *Am J Pathol* 80:129–142
- Okamoto K, Aoki K (1963) Development of a strain of spontaneously hypertensive rats. *Jpn Circ J* 27:282–293
- Koletsky S (1973) Obese spontaneously hypertensive rats—a model for study of atherosclerosis. *Exp Mol Pathol* 19:53–60
- Michaelis OE 4th, Ellwood KC, Judge JM, Schoene NW, Hansen CT (1984) Effect of dietary sucrose on the SHR/N-corpulent rat: a new model for insulin-independent diabetes. *Am J Clin Nutr* 39:612–618
- Takaya K, Ogawa Y, Hiraoka J, Hosoda K, Yamori Y, Nakao K, Koletsky RJ (1996) Nonsense mutation of leptin receptor in the obese spontaneously hypertensive Koletsky rat. *Nat Genet* 14:130–131
- Kawai K, Sakairi T, Harada S, Shinozuka J, Ide M, Sato H, Tanaka M, Toriumi W, Kume E (2012) Diet modification and its influence on metabolic and related pathological alterations in the SHR/NDmcr-cp rat, an animal model of the metabolic syndrome. *Exp Toxicol Pathol* 64:333–338
- Hussein G, Nakagawa T, Goto H, Shimada Y, Matsumoto K, Sankawa U, Watanabe H (2007) Astaxanthin ameliorates features of metabolic syndrome in SHR/NDmcr-cp. *Life Sci* 80:522–529
- Marchesini G, Brizi M, Bianchi G, Tomassetti S, Bugianesi E, Lenzi M, McCullough AJ, Natale S, Forlani G, Melchionda N (2001) Nonalcoholic fatty liver disease: a feature of the metabolic syndrome. *Diabetes* 50:1844–1850
- Wei Y, Wang D, Topczewski F, Pagliassotti MJ (2006) Saturated fatty acids induce endoplasmic reticulum stress and apoptosis independently of ceramide in liver cells. *Am J Physiol Endocrinol Metab* 291:E275–E281
- Akazawa Y, Cazanave S, Mott JL, Elmi N, Bronk SF, Kohno S, Charlton MR, Gores GJ (2010) Palmitoleate attenuates palmitate-induced Bim and PUMA up-regulation and hepatocyte lipopoptosis. *J Hepatol* 52:586–593
- Li ZZ, Berk M, McIntyre TM, Feldstein AE (2009) Hepatic lipid partitioning and liver damage in nonalcoholic fatty liver disease: role of stearoyl-CoA desaturase. *J Biol Chem* 284:5637–5644
- Tanaka S, Yagi Y, Yamazaki T, Mitsumoto A, Kobayashi D, Kudo N, Kawashima Y (2012) Characterization of fatty acid profile in the liver of SHR/NDmcr-cp (cp/cp) rats, a model of the metabolic syndrome. *Biol Pharm Bull* 35:184–191
- Bligh EG, Dyer WJ (1959) A rapid method of total lipid extraction and purification. *Can J Biochem Physiol* 37:911–917
- Imai K, Koyama M, Kudo N, Shirahata A, Kawashima Y (1999) Increase in hepatic content of oleic acid induced by dehydroepiandrosterone in the rat. *Biochem Pharmacol* 58:925–933
- Yamazaki T, Wakabayashi M, Ikeda E, Tanaka S, Sakamoto T, Mitsumoto A, Kudo N, Kawashima Y (2012) Induction of 1-acylglycerophosphocholine acyltransferase genes by fibrates in the liver of rats. *Biol Pharm Bull* 35:1509–1515
- Zurkowski P (1964) A rapid method for cholesterol determination with a single reagent. *Clin Chem* 10:451–453
- Rouser G, Siakotos AN, Fleischer S (1966) Quantitative analysis of phospholipids by thin-layer chromatography and phosphorus analysis of spots. *Lipids* 1:85–86
- Flowers MT, Groen AK, Oler AT, Keller MP, Choi Y, Schueler KL, Richards OC, Lan H, Miyazaki M, Kuipers F, Kendziorski CM, Ntambi JM, Attie AD (2006) Cholestasis and hypercholesterolemia in SCD1-deficient mice fed a low-fat, high-carbohydrate diet. *J Lipid Res* 47:2668–2680
- Keppler D, Decker K (1974) Glycogen: determination with amyloglucosidase. In: Bergmeyer HU (ed) *Methods of enzymatic analysis*, Academic Press, New York
- Özcan U, Yilmaz E, Özcan L, Furuhashi M, Vaillancourt E, Smith RO, Görgün CZ, Hotamisligil GS (2006) Chemical chaperones reduce ER stress and restore glucose homeostasis in a mouse model of type 2 diabetes. *Science* 313:1137–1140

21. Lowry OH, Rosebrough NJ, Farr AL, Randall RJ (1951) Protein measurement with the folin phenol reagent. *J Biol Chem* 193:265–275
22. Nepokroeff CM, Lakshmanan MR, Porter JW (1975) Fatty acid synthase from rat liver. In: Lowenstein JM (ed) *Methods in enzymology*, Academic Press, New York
23. Karahashi M, Ishii F, Yamazaki T, Imai K, Mitsumoto A, Kawashima Y, Kudo N (2013) Up-regulation of stearyl-CoA desaturase 1 increases liver MUFA content in obese Zucker but not Goto-Kakizaki rats. *Lipids* 48:457–467
24. Tanaka T, Hosaka K, Hoshimaru M, Numa S (1979) Purification and properties of long-chain acyl-coenzyme-A synthetase from rat liver. *Eur J Biochem* 98:165–172
25. Yamada K, Okuyama H (1978) Selectivity of diacylglycerophosphate synthesis in subcellular fractions of rat liver. *Arch Biochem Biophys* 190:409–420
26. Bell RM, Miller Y (1976) A highly sensitive assay for microsomal diacylglycerol acyltransferase activity from isolated fat cells. *Anal Biochem* 71:436–443
27. Sheng Z, Otani H, Brown MS, Goldstein JL (1995) Independent regulation of sterol regulatory element-binding proteins 1 and 2 in hamster liver. *Proc Natl Acad Sci USA* 92:935–938
28. Krumdieck CL, dos Santos JE, Ho KJ (1980) A new instrument for the rapid preparation of tissue slices. *Anal Biochem* 104:118–123
29. Iritani N, Yamashita S, Numa S (1976) Dietary control of triglyceride and phospholipid synthesis in rat liver slices. *J Biochem* 80:217–222
30. Friedman MI, Harris RB, Ji H, Ramirez I, Tordoff MG (1999) Fatty acid oxidation affects food intake by altering hepatic energy status. *Am J Physiol* 276:R1046–R1053
31. Targher G (2007) Non-alcoholic fatty liver disease, the metabolic syndrome and the risk of cardiovascular disease: the plot thickens. *Diabet Med* 24:1–6
32. Roden M (2006) Mechanisms of disease: hepatic steatosis in type 2 diabetes—pathogenesis and clinical relevance. *Nat Clin Pract Endocrinol Metab* 2:335–348
33. Jump DB (2011) Fatty acid regulation of hepatic lipid metabolism. *Curr Opin Clin Nutr Metab Care* 14:115–120
34. Wang Y, Botolin D, Xu J, Christian B, Mitchell E, Jayaprakasam B, Nair M, Peters JM, Busik J, Olson LK, Jump DB (2006) Regulation of hepatic fatty acid elongase and desaturase expression in diabetes and obesity. *J Lipid Res* 47:2028–2041
35. Shimomura I, Bashmakov Y, Horton JD (1999) Increased levels of nuclear SREBP-1c associated with fatty livers in two mouse models of diabetes mellitus. *J Biol Chem* 274:30028–30032
36. Benhamed F, Denechaud PD, Lemoine M, Robichon C, Moldes M, Bertrand-Michel J, Ratzui V, Serfaty L, Housset C, Capeau J, Girard J, Guillou H, Postic C (2012) The lipogenic transcription factor ChREBP dissociates hepatic steatosis from insulin resistance in mice and humans. *J Clin Invest* 122:2176–2194
37. Elam MB, Wilcox HG, Cagen LM, Deng X, Raghov R, Kumar P, Heimberg M, Russell JC (2001) Increased hepatic VLDL secretion, lipogenesis, and SREBP-1 expression in the corpulent JCR:LA-cp rat. *J Lipid Res* 42:2039–2048
38. Shimomura I, Matsuda M, Hammer RE, Bashmakov Y, Brown MS, Goldstein JL (2000) Decreased IRS-2 and increased SREBP-1c lead to mixed insulin resistance and sensitivity in livers of lipodystrophic and ob/ob mice. *Mol Cell* 6:77–86
39. Glatz JF, Luiken JJ, Bonen A (2010) Membrane fatty acid transporters as regulators of lipid metabolism: implications for metabolic disease. *Physiol Rev* 90:367–417
40. Lewis GF (1997) Fatty acid regulation of very low density lipoprotein production. *Curr Opin Lipidol* 8:146–153
41. Delgado TC, Pinheiro D, Caldeira M, Castro MM, Gerald CF, López-Larubia P, Cerdán S, Jones JG (2009) Sources of hepatic triglyceride accumulation during high-fat feeding in the healthy rat. *NMR Biomed* 22:310–317
42. Donnelly KL, Smith CI, Schwarzenberg SJ, Jessurun J, Boldt MD, Parks EJ (2005) Sources of fatty acids stored in liver and secreted via lipoproteins in patients with nonalcoholic fatty liver disease. *J Clin Invest* 115:1343–1351
43. Jamdar SC, Cao WF (1995) Triacylglycerol biosynthetic enzymes in lean and obese Zucker rats. *Biochim Biophys Acta* 1255:237–243
44. Wendel AA, Lewin TM, Coleman RA (2009) Glycerol-3-phosphate acyltransferases: rate limiting enzymes of triacylglycerol biosynthesis. *Biochim Biophys Acta* 1791:501–506
45. Hammond LE, Neschen S, Romanelli AJ, Cline GW, Ilkayeva OR, Shulman GI, Muoio DM, Coleman RA (2005) Mitochondrial glycerol-3-phosphate acyltransferase-1 is essential in liver for the metabolism of excess acyl-CoAs. *J Biol Chem* 280:25629–25636
46. Cha JY, Repa JJ (2007) The liver X receptor (LXR) and hepatic lipogenesis. i: the carbohydrate-response element-binding protein is a target gene of LXR. *J Biol Chem* 282:743–751
47. Liu Q, Siloto RM, Lehner R, Stone SJ, Weselake RJ (2012) Acyl-CoA:diacylglycerol acyltransferase: molecular biology, biochemistry and biotechnology. *Prog Lipid Res* 51:350–377
48. Man WC, Miyazaki M, Chu K, Ntambi J (2006) Colocalization of SCD1 and DGAT2: implying preference for endogenous monounsaturated fatty acids in triglyceride synthesis. *J Lipid Res* 47:1928–1939
49. Miyazaki M, Kim YC, Ntambi JM (2001) A lipogenic diet in mice with a disruption of the stearyl-CoA desaturase 1 gene reveals a stringent requirement of endogenous monounsaturated fatty acids for triglyceride synthesis. *J Lipid Res* 42:1018–1024
50. Miyazaki M, Flowers MT, Sampath H, Chu K, Oztelberger C, Liu X, Ntambi JM (2007) Hepatic stearyl-CoA desaturase-1 deficiency protects mice from carbohydrate-induced adiposity and hepatic steatosis. *Cell Metab* 6:484–496
51. Vial G, Dubouchaud H, Leverve XM (2010) Liver mitochondria and insulin resistance. *Acta Biochim Pol* 57:389–392
52. Stefanovic-Racic M, Perdomo G, Mantell BS, Sipula II, Brown NF, O'Doherty RM (2008) A moderate increase in carnitine palmitoyltransferase 1a activity is sufficient to substantially reduce hepatic triglyceride levels. *Am J Physiol Endocrinol Metab* 294:E969–E977
53. Wu JW, Wang SP, Alvarez F, Casavant S, Gauthier N, Abed L, Soni KG, Yang G, Mitchell GA (2011) Deficiency of liver adipose triglyceride lipase in mice causes progressive hepatic steatosis. *Hepatology* 54:122–132
54. Stefan N, Kantartzis K, Häring HU (2008) Causes and metabolic consequences of fatty liver. *Endocr Rev* 29:939–960
55. Fu S, Yang L, Li P, Hofmann O, Dicker L, Hide W, Lin X, Watkins SM, Ivanov AR, Hotamisligil GS (2011) Aberrant lipid metabolism disrupts calcium homeostasis causing liver endoplasmic reticulum stress in obesity. *Nature* 473:528–531
56. Özcan U, Cao Q, Yilmaz E, Lee AH, Iwakoshi NN, Özdelen E, Tuncman G, Görgün C, Glimcher LH, Hotamisligil GS (2004) Endoplasmic reticulum stress links obesity, insulin action, and type 2 diabetes. *Science* 306:457–461
57. Ferré P, Fougère F (2007) SREBP-1c transcription factor and lipid homeostasis: clinical perspective. *Horm Res* 68:72–82
58. Issandou M, Bouillot A, Brusq JM, Forest MC, Grillot D, Guillard R, Martin S, Michiels C, Sulpice T, Daugan A (2009) Pharmacological inhibition of stearyl-CoA desaturase 1 improves insulin sensitivity in insulin-resistant rat models. *Eur J Pharmacol* 618:28–36
59. Matsuzaka T, Shimano H, Yahagi N, Kato T, Atsumi A, Yamamoto T, Inoue N, Ishikawa M, Okada S, Ishigaki N, Iwasaki H, Iwasaki Y, Karasawa T, Kumadaki S, Matsui T, Sekiya M, Ohashi K, Hasty AH, Nakagawa Y, Takahashi A, Suzuki H,

- Yatoh S, Sone H, Toyoshima H, Osuga J, Yamada N (2007) Crucial role of a long-chain fatty acid elongase, Elov16, in obesity-induced insulin resistance. *Nat Med* 13:1193–1202
60. Kammoun HL, Chabanon H, Hainault I, Luquet S, Magnan C, Koike T, Ferré P, Foufelle F (2009) GRP78 expression inhibits insulin and ER stress-induced SREBP-1c activation and reduces hepatic steatosis in mice. *J Clin Invest* 119:1201–1215
61. Listenberger LL, Han X, Lewis SE, Cases S, Farese RV Jr, Ory DS, Schaffer JE (2003) Triglyceride accumulation protects against fatty acid-induced lipotoxicity. *Proc Natl Acad Sci USA* 100:3077–3082
62. Trauner M, Arrese M, Wagner M (2009) Fatty liver and lipotoxicity. *Biochim Biophys Acta* 1801:299–310
63. Kohjima M, Higuchi N, Kato M, Kotoh K, Yoshimoto T, Fujino T, Yada M, Yada R, Harada N, Enjoji M, Takayanagi R, Nakamura M (2008) SREBP-1c, regulated by the insulin and AMPK signaling pathways, plays a role in nonalcoholic fatty liver disease. *Int J Mol Med* 21:507–511
64. Diraison F, Dusserre E, Vidal H, Sothier M, Beylot M (2002) Increased hepatic lipogenesis but decreased expression of lipogenic gene in adipose tissue in human obesity. *Am J Physiol Endocrinol Metab* 282:E46–E51
65. Warensjö E, Risérus U, Vessby B (2005) Fatty acid composition of serum lipids predicts the development of the metabolic syndrome in men. *Diabetologia* 48:1999–2005
66. Bjermo H, Risérus U (2010) Role of hepatic desaturases in obesity-related metabolic disorders. *Curr Opin Clin Nutr Metab Care* 13:703–708
67. Araya J, Rodrigo R, Pettinelli P, Araya AV, Poniachik J, Videla LA (2010) Decreased liver fatty acid delta-6 and delta-5 desaturase activity in obese patients. *Obesity* 18:1460–1463
68. Elizondo A, Araya J, Rodrigo R, Poniachik J, Csendes A, Maluenda F, Díaz JC, Signorini C, Sgherri C, Comporti M, Videla LA (2007) Polyunsaturated fatty acid pattern in liver and erythrocyte phospholipids from obese patients. *Obesity* 15:24–31